PHYSICAL AND CHEMICAL RESISTANCE OF ELASTOMERS IN CARBON DIOXIDE-LOADED AQUEOUS MONOETHANOLAMINE SOLUTIONS DURING AMINE-BASED CARBON DIOXIDE CAPTURE

A Thesis

Submitted to the Faculty of Graduate Studies and Research

In Partial Fulfillment of the Requirements

For the Degree of

Master of Applied Science

In

Process Systems Engineering

University of Regina

By

Wayuta Srisang

Regina, Saskatchewan

November 2013

UNIVERSITY OF REGINA

FACULTY OF GRADUATE STUDIES AND RESEARCH

SUPERVISORY AND EXAMINING COMMITTEE

Wayuta Srisang, candidate for the degree of Master of Applied Science in Process Systems Engineering**,** has presented a thesis titled, ***Physical and Chemical Resistance of Elastomers in Carbon Dioxide-Loaded Aqueous Monoethanolamine Solutions During Amine-Based Carbon Dioxide Capture,*** in an oral examination held on November 14, 2013. The following committee members have found the thesis acceptable in form and content, and that the candidate demonstrated satisfactory knowledge of the subject material.

External Examiner:	Dr. Farshid Torabi, Petroleum Systems Engineering
Co-Supervisor:	Dr. Raphael Idem, Process Systems Engineering
Co-Supervisor:	Dr. Terradet Supap, Adjunct
Committee Member:	Dr. Paitoon Tontiwachwuthikul, Process Systems Engineering
Committee Member:	Dr. Hussameldin Ibrahim, Process Systems Engineering
Committee Member:	*Dr. Zhiwu Liang, Adjunct
Chair of Defense:	Dr. Nader Mobed, Department of Physics

*Not present at defense

ABSTRACT

Developing processes for the removal of carbon dioxide (CO_2), the most abundant greenhouse gas (GHG), has been of tremendous research interest due to the serious global warming problems associated with CO_2 emissions. Among other sources, CO_2 that is produced from human activities such as energy production (especially from large point sources) are the main targets for CO_2 emissions mitigation. One of the mature methods for CO_2 removal from low-pressure gas steams is absorption using a chemical solvent such as monoethanolamine (MEA). Most of the literature has focused on corrosion characteristics of equipment exposed to the MEA environment. However, the characteristics of small components used in such plants, such as seals, are scant.

This thesis research studied the chemical resistance of raw elastomers, namely, ethylene propylene diene monomers (EPDM), natural rubber (NR), isobutylene isoprene (IIR) and styrene butadiene (SBR) to aqueous solutions of MEA and MEA+CO_2 in order to understand how these would affect the corresponding commercial elastomers when used in the amine environment. The raw elastomers (EPDM, NR, IIR and SBR) were immersed in the solutions of molarities of 3, 5 and 7 as well as 5 M MEA with 0.16, 0.25, 0.5 mol CO_2/mol MEA for 30 days at 40 °C. After the completion of immersion, the raw elastomer specimens were investigated for their chemical resistance by measurement of mass change as well as chemical change, the latter of which used Fourier transform infrared spectroscopy (FTIR) for analysis. The impurity and MEA concentration in the solutions were determined by using High performance liquid chromatography (HPLC). Other physical properties such as density, viscosity and refractive index were also

measured. The results showed that SBR and NR had poor chemical resistance to the amine solution resulting in high percentage mass change. Moreover, they both reacted with aqueous solutions of MEA and MEA+CO_2 to form amide compounds on their surfaces. In contrast, EPDM and IIR had very insignificant mass changes after the immersion. Also, their chemical structures did not have any significant changes.

As raw EPDM and IIR revealed good chemical resistance to aqueous solutions of MEA and MEA+CO_2, it became essential to test the commercial EPDM and IIR which would actually be used in real applications. PTFE, well known for having excellent resistance to most chemicals, was also included as the benchmark. These commercial materials were exposed to MEA solution (5 M with 0.5 mol CO_2/mol MEA) at 40 and 120 °C for 30 days each. The specimens were then analyzed for changes in mass, hardness and tensile strength. The results showed that PTFE was the most compatible with the solution at both 40 and 120 °C compared to EPDM and IIR as the mass, hardness and tensile strength of PTFE remained the same before and after the immersion. For EPDM and IIR, the mass slightly increased while hardness and tensile strength slightly decreased after the immersion at 40 °C. At 120 °C, the mass changes of EPDM and IIR were significantly higher than those of the elastomers before immersion. This was attributed to the absorption of liquid into the elastomers which brought about the reduction of hardness and tensile strengths of EPDM and IIR. In conclusion, PTFE is the most recommended to be used in any part of the CO_2 absorption process with amines (e.g. MEA). EPDM and IIR can be used in the absorber as it operates at low temperatures. However, in the regenerator column, EPDM and IIR are not recommended.

ACKNOWLEDGEMENTS

I would like to express my gratitude to Dr. Raphael Idem, my supervisor, for giving me the opportunity to pursue my graduate education. His technical suggestions and constructive advice were invaluable in guiding me and keeping me on the right track. I would like to acknowledge Dr. Teeradet Supap, my co-supervisor, for his tremendous support, guidance, and encouragement throughout my thesis research. I greatly appreciate the time and effort he has put on me and this thesis.

I would like to express my appreciation for the support I received during the course of my Master's program from my mentors, colleagues, friends and family. Without their support, I would never have completed this thesis.

I wish to thank my colleagues and friends at ITC, and to Ms. Robyn Fahlman for her technical support and friendship. I am greatly thankful to Dr. Ian Coulson of the Department of Geology for letting me use his equipment. Thanks are also given to the Engineering Workshop and Science store, both at the University of Regina, for their assistance whenever I had equipment difficulties or shortage of chemical supplies.

Finally, I gratefully acknowledge the Faculty of Graduate Studies and Research, University of Regina, for providing me with financial support along with International Test for CO_2 Capture (ITC), University of Regina, which provided me equipment and facilities for my research.

DEDICATION

I would like to express my enormous appreciation to my parents, Mr. Suriyatep and Mrs. Laddawan Srisang, for their endless love, support and encouragement. There were times I secretly felt discouraged and doubted myself and my ability but the pride and belief they have in me helped push me to move forward. Without their support, I would never have accomplished any of my achievements. I wish to thank Mr. Wilfred, who edited my thesis, and Mrs. Laura Olson, my host family, for taking care of me as one of their family members and for providing unwavering support. Without them, living and studying far away from home would be very difficult. Special thanks are given to Mr. Wichitpan Wrongwong, my boyfriend, for his understanding, sharing all the moment of happiness and sorrow, and also for providing some technical suggestions.

TABLE OF CONTENTS

Page

CHAPTER II: THEORY AND LITERATURE REVIEW

CHAPTER III: EXPERIMENTS

LIST OF TABLES

LIST OF FIGURES

NOMENCLATURE AND ABBREVIATIONS

°C	Temperature in degree Celsius
cm^{-1}	Wavenumver
F	Temperature in Fahrenheit
Hp	Horse power
kV	kilo volt
M	Molarity (mol/L)
ml	Milliliter
MPa	Mega Pascal
wt%	Percent weight

Abbreviations

AHPD	2-amino-2-hydroxymethyl-1,3-propanediol
ATR-FTIR	Attentuated total reflectance fourier transform infrared
CH_4	Methane
CFCs	Fluorocarbons
CO	Carbon monoxide
CO_2	Carbon dioxide
Cr	Chromium
CR	Chloroprene rubber
DAD	Diode Array detector
DEA	Diethanolamine

ENB	Ethylidene norbornene
EPA	Environmental Protection Agency
EPDM	Ethylene Propylene Diene Monomers
FTIR	Fourier transform infrared
GWP	Global Warming Potential
H_2	Hydrogen
HCl	Hydrochloric acid
HF	Hydrofluoric acid
HPLC	High Performance Liquid Chromatography
H_3PO_4	Phosphoric acid
H_2O	Water
H_2SO_4	Sulfuric acid
IEA	International Energy Agency
IIR	Isobutylene Isoprene Rub
IPCC	Intergovernmental Panel on Climate Change
KBr	Potassium bromide
KH_2PO_4	Potassium phosphate monobasic
LDPE	Low density polyethylene
MDEA	Methyldiethanolamine
MEA	Monoethanolamine
MEK	Methyl ethyl ketone
N_2	Nitrogen
NaCl	Sodium chloride

NBR	Nitrile rubber
NMR	Nuclear Magnetic Resonance
NO_2	Nitrous oxide
NR	Natural Rubber
O_2	Oxygen
O_3	Ozone
PEM	Proton exchange membrane
PIP	Piperidine
PTFE	Polytetrafluoroethylene
PVA	Polyvinyl alcohol
PZ	Piperazine
RID	Refractive index detector
SBR	Styrene Butadiene Rubber
SEM	Scanning Electron Microscope
SiO_2	Silicon oxide
TEA	Triethanolamine

CHAPTER I

INTRODUCTION AND BACKGROUND

This chapter provides the background on a global environmental problem known as climate change. It focuses on the effect of carbon dioxide (CO_2) emissions on global warming as well as CO_2 capture technologies to mitigate the emissions. Importantly, it looks at the motivation behind the current research which looks at the often forgotten issue of the compatibility of elastomeric materials that are used as seals in the CO_2 capture process. These are explained in terms of their importance and proper selection. Lastly, this chapter also includes the objectives and scope of this research.

1.1 Global Warming and CO_2 Emissions

In the past century, the world average temperature has increased by 1.4 ^oF (0.78 ^oC) annually and it is likely to rise another 2 ^oF (1.11 ^oC) each year in the next century, as reported by Environmental Protection Agency (EPA). This phenomenon is known as global warming, which leads to climate change. The increase in temperature of 1 or 2 ^oF each year appears to be very small. However, it can result in a large impact on the world climate. Changes in rainfall patterns, the frequency of floods, droughts, higher temperatures, and more acidity of ocean waters are all evidence of climate change due to this small increase in world average temperature. Most climatologists believe that global warming is essentially caused by the so-called greenhouse gases (GHGs) that absorb heat and prevent it from escaping back into space (Piewkhaow, 2011). This leads to the warming of the planet's surface.

GHGs such as CO_2, methane (CH_4), water vapor (H_2O) and ozone (O_3) occur in nature while some fraction of these gases (especially CO_2 and CH_4) as well as other greenhouse gases such as nitrous oxide (NO_2) and fluorocarbons (CFCs) are produced by human activities. How aggressive each GHG is in absorbing heat is reported as Global Warming Potential (GWP), the ability of any GHG to trap heat in the atmosphere as compared to CO_2. The GWP of CH_4, NO_2 and CFCs are 25, 298, and 22800 times higher than the GWP of CO_2 (IPCC, 2007). Even though the GWP of CO_2 gas is very low compared to other GHGs, CO_2 accounts for 84% of all GHGs added to the atmosphere as shown in Figure 1.1, and it is therefore clear that reducing CO_2 emissions holds significant potential in the effort to solve global warming problems.

In 2009, 29 billion tons of CO_2 were released, as reported by the International Energy Agency (IEA) in 2011. As illustrated in Figure 1.2, the attribution to CO_2 emissions decreases in the order: electricity and heat > transportation > and industry with shares of 41, 23, and 20%, respectively. Regrettably, a new record revealed by Germany's renewable energy institute, has shown that global CO_2 emissions increased to 34 billion tons in 2011. If this trend is sustained, CO_2 emissions worldwide could reach 40 million tons in 2020. Figure 1.2 also shows that the dominant sources of CO_2 are the production of electricity and heat, and transportation. In order to reduce the CO_2 released from transportation, alternative fuels such as hydrogen or electricity could be used in many vehicles. Although hydrogen and electricity production can also result in the release of CO_2, it can be captured at the plant where it is produced.

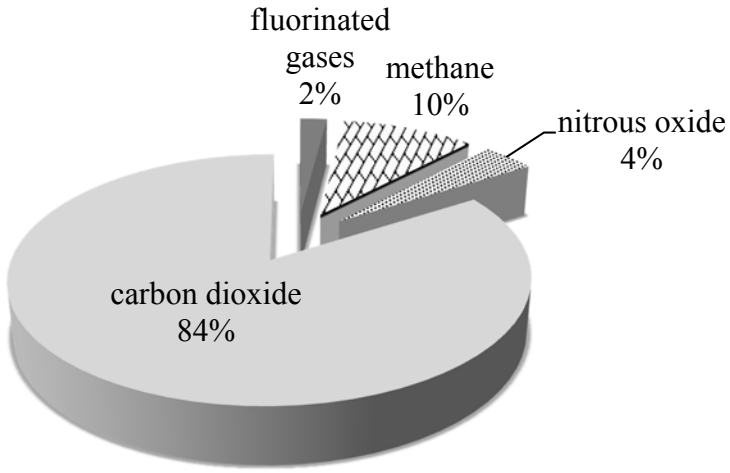

Figure 1.1 Greenhouse gas emissions in 2009 (IEA, 2011)

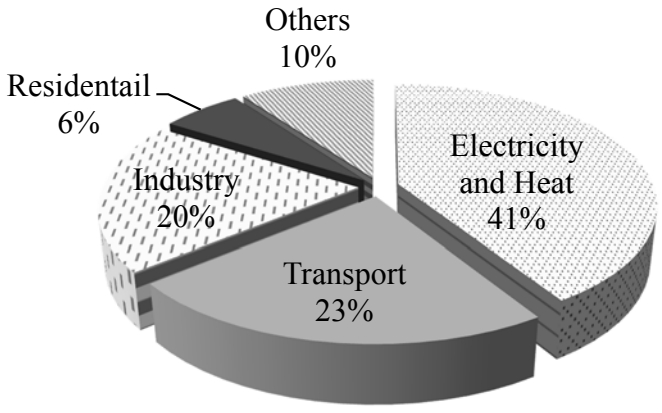

Figure 1.2 Emission of CO_2 from fossil fuel used in 2009 (IEA, 2011)

1.2 Approaches to CO_2 Capture

The concern about global warming has spurred interest in the capture of CO_2 at its source, especially in power generation industries which are a large source of CO_2 emissions. Power generation systems that have low CO_2 emission have been researched and developed by many researchers. Also, three main approaches for reducing CO_2 emission from power generation plants existing today are being investigated. These are oxy-fuel combustion, pre-combustion CO_2 capture, and post-combustion CO_2 capture (Wang et al., 2011).

1.2.1 Oxy-Fuel Combustion

The traditional coal combustion burns coal using air, which produces a large amount of nitrogen (N_2) in the flue gas, thereby necessitating the separation of CO_2 from N_2 as practiced in the post combustion process. Oxy-fuel is an alternative way by which pure oxygen (O_2) is used instead of air in the combustion process so that the resulting syngas will contain mostly steam and CO_2. These two components can be separated easily by cooling and the condensation of water. The purity of CO_2 capture can range up to 100% in this process; however, it is still very expensive to obtain pure O_2 that is required in the process. Two interesting O_2 and N_2 separation techniques from air available today are cryogenic separation of air and membrane separation (Scheffkenecht et al, 2011).

1.2.2 Pre-Combustion CO_2 Capture

As the name implies, pre-combustion capture is the process in which CO_2 is captured before combustion. The process starts with the conversion of fuel to syngas, a mixture of hydrogen (H_2) and carbon monoxide (CO), by the traditional gasification process. Then CO undergoes the water gas shift reaction, which is a mildly exothermic reaction between CO and steam (H_2O) to form CO_2 and H_2. The mixture of CO_2 and H_2 is separated in a manner similar to that used in post combustion capture. The H_2 obtained can be used both in power plants and as fuel in vehicles where its combustion does not produce CO_2 emissions. Pre-combustion CO_2 capture can reduce emissions of CO_2 by 90%. However, existing power plants would require significant modification to use this process. As such, it would be suitable only for new power plants (Andersen, 2005).

1.2.3 Post Combustion CO_2 Capture

A post combustion process refers to the capture of CO_2 after combustion. It is a major approach for CO_2 capture today because it has several advantages over the other two approaches. For example, post combustion technology is applicable to the majority of existing plants, while pre combustion and oxy fuel would be applicable to only new plants. In the post combustion process, flue gas contains mainly N_2, O_2 and a low concentration of CO_2 which is typically 10 to 15% at a pressure near atmospheric (Herzog, 2009). The partial pressure of CO_2 in this stream is low, and therefore, there are limited technologies that can be used for separation of CO_2 from this stream. Generally, technologies such as adsorption, absorption, membrane separation, and cryogenic separation can be applied to this process. However, in a low partial pressure system, the

best way and most popular technology is absorption using a chemical solvent (Hoff, 2003).

In general, the CO_2 chemical absorption process consists of two main vessels: an absorber and a regenerator, as shown in Figure 1.3. In an absorber, a stream of flue gas is introduced into the bottom of the column. The flue gas flows upward to make countercurrent contact with a liquid absorbent that is fed from the top of the column. The CO_2 transfers from the gas phase to the liquid phase through the phase boundary due to concentration difference. The CO_2 both physically dissolves and chemically reacts with the absorbent. As the CO_2 transfers from the flue gas into the liquid absorbent, the absorbent solution becomes more concentrated with CO_2 and is called "rich solution". The rich solution is collected at the bottom of the absorber and pumped through a heat exchanger to pre-heat the solution before feeding it to the top of a regenerator where it is heated and regenerated.

In the regenerator, the rich solution is supplied with additional heat, typically in the form of low pressure steam. The heat results in the CO_2 coming out of solution as the solution falls to the bottom of the regenerator. The solution, now with a low CO_2 concentration, is called "lean solution" and is collected at the bottom of the regenerator and pumped through the heat exchanger to be cooled down before it is fed back to the absorber. The stripped CO_2 gas from the top of the regenerator is collected, compressed and transported to storage (Wang et al., 2011).

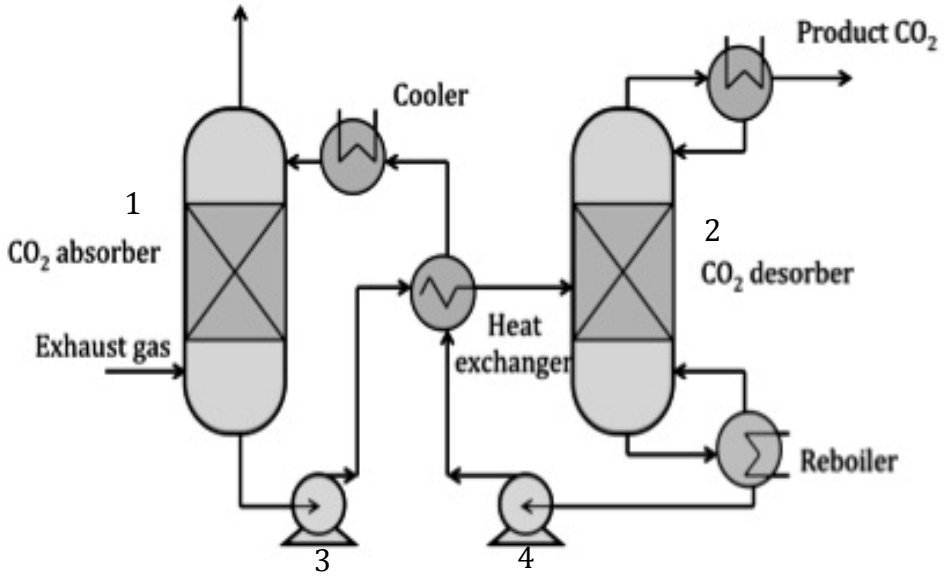

Figure 1.3 Typical process diagram of CO_2 absorption using chemical solvents

Table 1.1 Typical operating temperatures in CO_2 absorption plants using MEA

Number	Equipment	Temperature (°C)
1	Absorber	30-70
2	Regenerator	120
3	Pump	30-70
4	Pump	120

1.3 Solvents for CO_2 Absorption

Solvents for CO_2 absorption are generally categorized into two groups: 1) chemical solvents and 2) physical solvents. The selection of proper solvent (chemical or physical) depends on many factors, including the purity of treated gas, volume of the gas stream, condition of feed gas (partial pressure of CO_2), operating conditions of CO_2 capture process such as pressure and temperature, and the quality of the CO_2 product.

For physical absorption, interaction between the solvent and CO_2 is very weak. Therefore, CO_2 dissolves into the physical solvent without any chemical reaction occurring. The regeneration of the solvent can be done simply by reducing pressure, which requires much lower energy consumption compared to chemical solvents. However, the physical solvent is particularly suitable when the gas stream has a high concentration of CO_2 (15-60%) and is at a high pressure (2-7 MPa) as this provides a large driving force for mass transfer (Rubin, 2005). This condition is usually found in natural gas separation processes. The typical physical solvents used are water, Rectisol (methanol) and Selexol (dimethyl ether of polyethylene glycol) (Wang et al., 2011).

In the case of gases near atmospheric pressure and with a relatively low partial pressure of CO_2 such as in flue gases from power generation plants, it is preferable to use a chemical solvent in the capture process. The chemical reactions that occur within the absorbent transform the CO_2 into other compounds and enhance the driving force for the mass transfer.

CO_2 is an acidic gas; therefore, absorbents used to remove CO_2 from gas streams are basic solutions, such as sodium hydroxide, sodium bicarbonate, or amine solutions. After dissolving into the solution, CO_2 chemically reacts with the chemical solvents

reversibly or irreversibly. The chemical solvents that reversibly react with CO_2 are more favored because they can be regenerated and reused in the process. Among these absorbents, amines, especially MEA, have been a popular choice for CO_2 gas absorption. This thesis focuses on the compatibility of elastomer seals with the solvent used in low pressure CO_2 capture for power generation plants.

1.4 Elastomer Seals

Seals can be made from various materials, such as fibrous, metallic and elastomer (ESA, 1998). Among them, elastomer is the most commonly used due to its elasticity, low cost, and a wide variety of available chemical structures. The elasticity of elastomers differentiates it from other materials as it can be compressed between gaps that must be sealed. However, simple elastomers alone cannot be effective seals. Other ingredients or additives, such as fillers or vulcanizing agents are added to make the elastomer easier to process or to improve the elastomer's physical or chemical properties. The combination of elastomer and additives is called elastomeric compound. Fillers (i.e. black carbon, silica) are added in the compound in order to reinforce, extend the material, and reduce cost. Vulcanizing agents or curing agents help elastomers to vulcanize or crosslink to improve their strength. Accelerators and inhibitors are added in order to control the reaction in the process of vulcanization. Other additives might include plasticizers to improve flexibility, and pigment for colorization and to reduce degradation in environments such as O_2 or radiation (Ciesielski, 1999).

In the CO_2 absorption by MEA process, as in many other processes, elastomer seals are used to prevent leakage of MEA solution. Various elastomer seals are installed

in many places including within columns, piping, and pumps. The absorption and regeneration columns in CO_2 capture process by MEA are usually recommended to be made from low carbon steel which is believed to have high chemical resistance (Wattanaphan, 2012). For absorber or regenerator columns with small diameter, two or more columns are normally connected in series in order to increase the productivity of the process. Moreover, these columns in series can be easily dismantled when maintenance is required. Between the columns, seals are placed to prevent leakage of the absorbent solution.

Piping is the main component of both the absorption and regenerator plants. Between flanges in pipes, seals, called gaskets, are placed and compressed to prevent the escape of MEA. Expansion joints are another location for elastomer seals to be used in piping. Prevention of stress in piping systems that could contribute to liquid leakage and a drop in system pressure can be accomplished by the use of expansion joints. These provide some flexibility and absorb dynamic movements of machinery and adjoining buildings etc. (Chandrasekaran, 2009).

Besides columns and piping, pumps are one of the important utilities used in CO_2 absorption process plants. A primary application is for the transfer of aqueous MEA between absorber and regenerator. Mechanical seals are installed on the shaft of pumps to prevent leaking of liquid from the housing. A leak of MEA from a pump contributes not only to the loss of absorbent CO_2 but also causes a decrease in pressure necessary to transfer the liquid (Chandrasekaran, 2009).

1.5 Research Motivation

Over the past decade, developing processes for removal of CO_2 from combustion gases has been of considerable interest due to the desire to mitigate a serious global warming problem. CO_2 absorption by chemical solvents such as MEA is one of the most favored methods for CO_2 removal from low-pressure gas streams due to its effectiveness and because the solvent MEA can be reused, thus lowering investment costs.

Considerable research effort has been directed to the study of the application of MEA for absorption of CO_2 in order to improve the process. The areas include kinetics of absorption (Aboudheir et al., 2003), degradation of MEA solution (Supap et al., 2006), mass transfer (Aroonwilas, Veawab, & Tontiwachwuthikul, 1999) and corrosion (Wattanaphan, 2012). On the other hand, there has only been limited work done on the study of the compatibility of materials being used in this process. Most work done on materials has been on corrosion studies which focuses only on metallic materials used in equipment that is exposed to MEA. Based on these studies, low carbon steel can only be recommended for use for equipment material such as columns, pipeline and valves under certain conditions (Wattanaphan, 2012). A literature search on the study of material compatibility for non metallic materials in CO_2 absorption plants, especially seals made from elastomers, shows that limited work has been done so far.

Any incompatibility between seals and liquid can shorten the seals' life resulting in leakage and the need for replacement of the seals. Even though seals are inexpensive, the replacement cost, time and labor can be extremely costly. Moreover, the leaking of seals can contribute to process outages, wasted energy, reduction of plant efficiency, environmental spills and personal injury (ESA, 1998). According to the report by John C.

Cox (business manager of Swagelok Company, Solon Ohio), leakage of fluid can cost industry millions of dollars every year. A company could waste fifty dollars per week from the selection of improper seal material (Chandrasekaran, 2009). Therefore, the selection of the right kind of elastomers needs to be made carefully to avoid the incompatibility between elastomers and liquids.

Currently, elastomer seal technologies are well developed and there are many commercial elastomer seals available. To select seals for use in a CO_2 capture process, compatibility tables provided by elastomer companies are the only data available. Compatibility tables rate the resistance of elastomers to various chemicals including some of the amines used in a CO_2 capture processes, such as MEA and DEA. However, these tables only provide data for amines at certain concentrations whereas the solvents are not composed of MEA alone in an actual CO_2 absorption process using MEA solutions. CO_2 dissolves and reacts with MEA during the absorption process, forming new compounds and changing the pH of the MEA solutions. These compounds and various pH levels have the potential to cause the degradation of the elastomers. In addition, the temperature of the MEA solution in this process is not constant but differs between the absorber and the regenerator. This implies that the data from compatibility tables is too simplistic and insufficient for selecting the right seal for use in a CO_2 absorption process. The usage of seal materials that cannot withstand amines in actual operating condition might cause seals failure and leakage of liquid from the process. Therefore, the compatibility of seals to be used in specific applications in the CO_2 absorption process needs to be evaluated.

In this thesis, the compatibility of elastomers (IIR, EPDM, SBR, NR, and PTFE) with MEA solutions used in the actual CO_2 absorption process was studied. The chemical resistance of the elastomers to different MEA concentrations (3, 5, 7 M) was also investigated. Moreover, the effect of CO_2 loading (0.16, 0.25, 0.5 mol CO_2/mol MEA in MEA 5 M) which varies throughout CO_2 absorption plants as well as the effect of temperature (40°C in absorber and 120°C in regenerator) were also determined.

1.6 Research Objectives

As mentioned previously, the compatibility between seals and MEA solutions is very important for prevention of MEA leakage and for performance of the process. This thesis aims to study the compatibility of material to be used in seal application in CO_2 capture using MEA. The factors considered for compatibility testing are the composition of the liquid medium (MEA concentration, CO_2 loading) and liquid temperature. The main research objective of this thesis and some details are given as follows:

1. Screen raw elastomers that are likely to withstand MEA solutions when used in a post-combustion CO_2 Capture process using reactive solvents. The initial screening is performed based on the data from compatibility tables that are published by elastomer suppliers.

2. Study the effect of MEA concentrations (3, 5, 7 M) and the effect of CO_2 loadings (0.16, 0.25, 0.5 mol CO_2/mol MEA in MEA 5 M) on the degradation of raw elastomers (IIR, EPDM, SBR, and NR). In order to find suitable elastomer seals, it needs to ensure that raw elastomers used can resist MEA solutions and MEA solutions loaded with CO_2.

3. Study the compatibility and the effect of temperature on the compatibility of commercial elastomers (IIR, EPDM and PTFE) in MEA with CO_2 loading solutions (0.5 molCO_2/mol MEA in 5 M MEA). The elastomers in commercial form are tested in order to ensure that their performance does not change as a result of the incorporation of fillers and additives. Moreover, the effect of temperature on the compatibility of seals is significant and is studied because in the actual CO_2 absorption by MEA, the temperatures typically vary from 40 to 120°C from absorber to stripper (Øi, 2007).

CHAPTER II

THEORY AND LITERATURE REVIEW

2.1 Overview of Amines Used in CO_2 Capture Process

The functional groups of amines include the amino group (-NH_2, NRH and NRR') and alcohol (-OH). For a number of decades, the amines have been used extensively for CO_2 capture at low partial pressure in flue gas due to their weak alkalinity provided by the amino group being favorable to chemical reaction with acidic CO_2. The absorption reactions typically form water soluble compounds with only weak chemical bonds which are essential for solvent regeneration. This constitutes one of the most important advantages of the amines. The chemical bonds between CO_2 and amines are easily broken by mild heating in the regeneration process (Mandal et al., 2001; Wang et al., 2004). Moreover, the hydroxyl group in the alkanolamines provides for a reduction of the partial pressure and an increase in water solubility (Kohl & Nielsen, 1997).

The commonly used alkanolamines in CO_2 capture processes are MEA, diethanolamine (DEA), methyldiethanolamine (MDEA). MEA, a primary amine, has been popular for CO_2 capture processes with relatively low CO_2 concentrations in the gas stream (e.g. power plants) due to its high reactivity (Hoff, 2003). However, the absorption capacity of MEA is limited by equilibrium stoichiometry at about 0.5 mole CO_2 per mole amine where carbamate is the final product (Mandal et al., 2001). Considering only the energy consumption of the regeneration process, MEA is not the most appealing solvent as the energy requirement for solvent regeneration is quite high compared to other amines such as MDEA (Chakma, 1995).

Table 2.1 Commonly used alkanolamines in CO_2 capture process

Alkanolamine	Structure
Monoethanolamine (MEA)	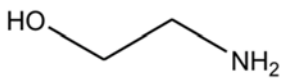
Diethanolamine (DEA)	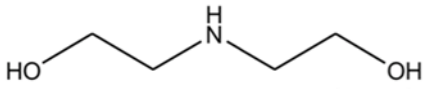
Methyldiethanolamine (MDEA)	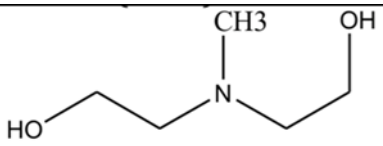

Even though MEA is not the ideal solvent for CO_2 capture after considering all the operational perspectives (rate of reaction, absorption capacity, and energy requirement for solvent regeneration), it is still one of the best solvents due to its high reactivity. This factor alone provides many benefits such as reduced size of equipment and low capital cost. Operation costs can also be minimized based on the reduction of equipment size and the smaller volume of solvent required.

The absorption mechanisms of CO_2 in aqueous MEA solution are shown below (Aboudheir et al., 2003):

Ionization of water

$$2H_2O \leftrightarrow OH^- + H_3O^+ \quad (2.1)$$

Dissociation of dissolved CO2 through carbonic acid to bicarbonate:

$$CO_2 + 2H_2O \leftrightarrow HCO_3^- + H_3O^+ \quad (2.2)$$

Bicarbonate formation

$$CO_2 + OH^- \leftrightarrow HCO_3^- \quad (2.3)$$

Dissociation of bicarbonate

$$HCO_3^- + H_2O \leftrightarrow CO_3^{2-} + H_3O^+ \quad (2.4)$$

Dissociation of protonated MEA

$$RNH_3^+ + H_2O \leftrightarrow RNH_2 + H_3O^+ \quad (2.5)$$

Zwitterion formation by the reaction of MEA with CO_2

$$CO_2 + RNH_2 \leftrightarrow RNH_2^+COO^- \quad (2.6)$$

Carbamate formation by deprotonation of zwitterion

$$RNH_2^+COO^- + RNH_2 \leftrightarrow RNH_3^+ + RNHCOO^- \quad (2.7)$$

$$RNH_2^+COO^- + H_2O \leftrightarrow RNH_3^+ + RNHCOO^- \quad (2.8)$$

$$RNH_2^+COO^- + OH^- \leftrightarrow RNH_3^+ + RNHCOO^- \quad (2.9)$$

$$RNH_2^+COO^- + HCO_3^- \leftrightarrow RNH_3^+ + RNHCOO^- \quad (2.10)$$

$$RNH_2^+COO^- + CO_3^{2-} \leftrightarrow RNH_3^+ + RNHCOO^- \quad (2.11)$$

Carbamate reversion to bicarbonate

$$RNHCOO^- + H_2O \leftrightarrow RNH_2 + HCO_3^- \quad (2.12)$$

2.2 Studies of Plant Materials Degradation in Amines Base CO_2 Capture

An important concern in CO_2 capture processes is the material corrosion and degradation that occurs in the process plants. Many researchers focus on the degradation by amine solvents when used with carbon steel material mainly used to construct the CO_2 capture plant. Kittel and co-workers observed that corrosion of carbon steel in a CO_2 capture plant using MEA occurred at a high temperature and CO_2 loading (Kittel et al., 2009). The deterioration of polymeric membranes, also used in amine based CO_2 capture process to help increase the contact area between CO_2 and amine solution, have also been investigated. Wang et al. (2004) investigated the impact of DEA on membrane surfaces during CO_2 capture in a membrane contactor. The polypropylene microporous hollow fiber membrane exposed to 20 and 30 wt% DEA solutions containing dissolved CO_2 gas was found to be damaged with increased surface roughness after the immersion period. A reaction between the membrane and DEA was suspected to occur causing the deterioration of the membrane surface. On the other hand, dissolved CO_2 was found to slow down the deformation process of the microporous membrane and helped to reduce the increase in surface roughness due to the formation of carbamate with DEA (Wang et al., 2004).

Franco et al. (2008) studied the interaction of MEA with polypropylene hollow fiber membrane after being used for CO_2 capture in a membrane contactor for 68 hours. It was discovered that the content of oxygen in polypropylene increased from 0.78% to 1.49% after the operation. The increased oxygen content was suspected to be due to the oxidation reaction of propylene. The reaction between membrane and amine (MEA) used in the capture plant was confirmed again by Sedghi et al. (2011) who studied the deterioration of low density polyethylene (LDPE) hollow fibers exposed to 30 wt% CO_2-loaded/unloaded MEA solutions. The LDPE that was kept immersed in the MEA solutions at 25 and 65 °C for 30 days was found to react with the aqueous MEA to form secondary amides observed as the amide I band (carbonyl functional group) and II band (bond between nitrogen and hydrogen) in FTIR spectra. The formation of amide was a result of auto oxidation of LDPE which contributed to the formation of –COOH groups, followed by reaction of –COOH groups and MEA resulting in the formation of secondary amides that was detected on the LDPE surface. Sedghi et al. (2011) proposed a reaction pathway of this phenomenon as follows.

$$PEOOH + NH_2CH_2CH_2OH \rightarrow PECONHCH_2CH_2OH \qquad (2.13)$$

The degree of deterioration increased with increasing temperature due to the effect of temperature in accelerating the reactions. On the other hand, an increase in CO_2 loading reduced the deterioration of LDPE. This was because the increased CO_2 loading reduced the pH of the loaded MEA solution which retarded the oxidation reaction of LDPE. Moreover, with the presence of CO_2 in the MEA loaded solutions, some MEA

was consumed to form a stable carbamate salt, which was more probable than the formation of amide groups (Sedghi et al., 2001).

Recently, Sedghi et al. (2012) expanded their work by studying the degradation of LDPE in MEA, 2-amino-2-hydroxymethyl-1,3-propanediol (AHPD), and piperazine (PZ) solutions. Similar test procedures were used for the solutions of MEA, AHPD, and mixtures of MEA/PZ and AHPD/PZ. The results showed that an increase of PZ concentration in both the MEA/PZ and AHPD/PZ solutions retarded the deterioration of LDPE for two reasons. Firstly, a higher concentration of PZ contributed to an increase in surface tension which helped to prevent the amine from easily penetrating the LDPE membrane pores. Secondly, a similar structure of PZ to piperidine (PIP), often used as a stabilizer for auto-oxidation in polymers, could have helped to retard the auto-oxidation process of the membrane (Mosadegh-Sedghi et al., 2012).

2.3 Elastomers used in Amines Based CO_2 Capture Units

Elastomers are one of the categories of polymers which have been used in a wide range of applications due to their superior elasticity. In general, a polymer has an amorphous structure above its transition temperature. Below this temperature, the polymer becomes crystalline and rigid. Unlike other classes of polymers that are viable either below their transition temperature or in the semi crystalline state, elastomers have a low glass transition temperature and are used above this temperature as amorphous polymers. Raw elastomers are typically soft, sticky and very sensitive to temperature. In order to make elastomers more appealing for industrial use, some additives are added

essentially to enhance the properties of the elastomer such as tensile strength, hardness, life expectancy and color (Schweitzer, 2010).

Initially, the selection of elastomers to be used in any specific application is commonly based on compatibility tables. Based on the compatibility tables of various elastomer manufacturers, this section chose to review specific elastomers suitable for use in the CO_2 absorption process using a reactive solvent, MEA, which is also the solvent used for the current research. The recommended elastomers for MEA are Natural Rubber (NR), Styrene Butadiene Rubber (SBR), Ethylene Propylene Diene Monomers (EPDM), Isobutylene Isoprene Rubber (IIR), and Polytetrafluoroethylene (PTFE).

2.3.1 Natural Rubber (NR)

NR is a biological homopolymer of methyl butadiene (cis-isoprene) obtained from the rubber tree. The chemical structure of NR is shown in Table 2.1. It is well known that NR has an excellent resistance to most inorganic salt solutions and alkalis but poor swelling resistance in oil and nonpolar solvents because the structure of cis-isoprene does not provide sufficient interlock in the polymer chains (Ciesielski, 1999). Georgoulis et al. (2005) mentioned that NR showed a high degree of swelling when it comes in contact with non polar solvents such as toluene. Baah and Baah (2005) immersed NR into malic acid for 30 days and found that the elastomer could absorb only a small amount of malic acid due to the difference in polarity between NR and malic acid.

2.3.2 Styrene Butadiene Rubber (SBR)

SBR is produced by copolymerization of styrene and butadiene monomers. SBR with its chemical structure shown also in Table 2.1 has poor weathering properties as it deteriorates in sunlight. However, the elastomer has a fair to good durability in acids, alkalis and alcohols. The major use of SBR is in the manufacture of automobile tires, conveyor belts, seals and gaskets.

2.3.3 Ethylene Propylene Diene Monomer (EPDM)

As shown in Table 2.1, EPDM is a terpolymer of ethylene, propylene and diene monomers. EPDM is a saturated, non-polar polymer even with diene embedded in its structure. It is well known that the diene monomer in EPDM plays a very important role in the process of vulcanization even though the concentration of the diene monomer in the polymer is very small; this thus makes EPDM to still maintain its saturated backbone and non-polar structure. According to Mitra et al. (2006), the most popular diene used in terpolymerization process is ethylidene norbornene (ENB). Due to the saturated backbone and non-polar nature of EPDM rubber, EPDM has a high electrical resistivity and excellent resistance to heat, oxidation, ozone, weather and chemicals. That is why EPDM is widely used in the production of seals and gaskets for many industrial applications (Ciesielski, 1999). Tan et al. (2009) studied the chemical stability of EPDM in an artificial proton exchange membrane (PEM) environment created by mixing 12 ppm of sulfuric acid (H_2SO_4) with 1.8 ppm of hydrofluoric acid (HF). The chemical and interfacial changes of the EPDM samples were investigated with Attentuated Total Reflectance Fourier Transform Infrared (ATR-FTIR) optical microscope. The results

showed that the main structural chain of EPDM was still relatively stable. No significant change in the rubber occurred except that silicon oxide (SiO_2) that was used as filler was released to the environment during immersion.

2.3.4 Isobutylene isoprene rubber (IIR)

IIR or butyl rubber is a synthetic polymer of isobutylene with a small amount of isoprene monomers (i.e. approximately 3%) (Dong, 2010). This small amount of isoprene is very important for the crosslinking process. On the other hand, the high content of isobutylene in IIR contributes to the formation of a side methyl chain along the polymer chain, which prevents permeation of air and liquid. IIR is very nonpolar and has exceptional resistance to chemicals such as dilute acid, alkalis, phosphate, ethylene and ethylene glycol. IIR structure is shown in Table 2.1.

2.3.5 Polytetrafluoroethylene (PTFE)

PTFE is well known under its trade name as Teflon by DuPont. It is in the category of a thermoplastic which is fully fluorinated, and in which hydrogen atoms in the polymer backbone are substituted by fluorine atoms, as shown in Table 2.2. The bonds between carbon and fluorine have high bond energy compared to the bonds of carbon and hydrogen. Therefore, PTFE has a low chemical reactivity and a high resistance to heat and chemical. These are the reasons that PTFE has been used for sealing and piping applications.

Table 2.2 Structure of elastomers

Elastomers	Structure
Natural Rubber (NR)	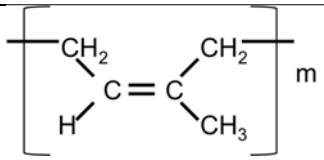
Styrene Butadiene Rubber (SBR)	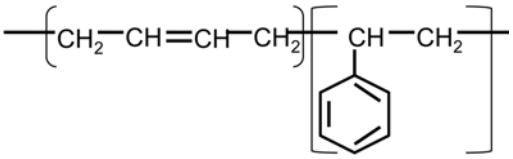
Ethylene Propylene Diene Monomer (EPDM)	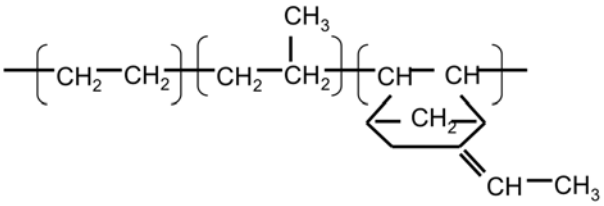
Isobutylene isoprene rubber (IIR)	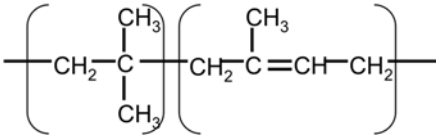
Polytetrafluoroethylene (PTFE)	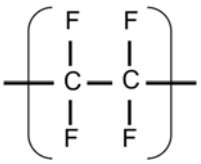

2.4 Elastomer Selection

The selection of an elastomer for a particular service must be made carefully in order to avoid rapid deterioration due to incompatibility with the plant fluid used (e.g. liquid amines used as absorbents in the CO_2 capture process).

2.4.1 Elastomer Selection Parameters

Generally, two important parameters needed to be considered are the compatibility of the elastomers with the plant liquid and the operating temperature at the location where the elastomers is used in the plant. When these two parameters are known, one can reliably recommend suitable elastomer polymer base.

2.4.1.1 Plant Liquid

If the selected elastomers and the plant liquid are not compatible, either a physical or a chemical interaction will occur. Physical absorption occurs when the elastomers absorb the liquid medium into its structure, thus contributing to the swelling of the elastomer. The elastomers can often return to their original state after the liquid medium environment is removed.

Baah and Baah (2001) studied the effect of acetaldehyde, acetic anhydride and malic acid on nitrile, neoprene and NR. The results showed that the mass of rubbers increased during immersion due to the absorption of the solvents (Baah and Baah, 2001). The principle of swelling of elastomers can be explained by their polarity and that of the liquid medium. For polar molecules, intermolecular forces called “dipole-dipole” are formed by contact between the negative end of liquid medium and the positive end of the elastomer (Haseeb et al, 2010). Georgoulis et al. (2005) studied the permeation of toluene

and methyl ethyl ketone (MEK) in NR, nitrile rubber (NBR) and polyvinyl alcohol (PVA) gloves. The results showed negligible permeation of the solvents through PVA. In contrast, the permeation strongly depended on the monomers and chemical structure of the solvents in NR and NBR gloves. A non-polar toluene permeated easily through NR containing non-polar monomers. On the other hand, a more polar MEK permeated more easily in NBR which was a polar polymer (Georgoulis, Morgan, Andrianopoulos, & Seferis, 2005).

When chemical interaction occurs, the results are different from those of physical absorption. The chemical reactions that occur might bring about structural changes to the elastomers. For example, the immersion of chloroprene rubber (CR) in biodiesel at room temperature can increase the amount of the carbonyl group formed in the elastomer (Haseeb et al., 2010). In the case of compound elastomers formulated with special additives for enhancement of physical properties), the incompatibility of liquid medium and elastomers can cause dissolution of plasticizers and other components in the elastomers, thus altering their performance (Ciesielski, 1999).

2.4.1.2 Temperature

The liquid temperature in the plant usually has an influence on the severity of deterioration of the elastomers. In general, liquid medium at a higher temperature is more corrosive to the elastomer. Moreover, chemical reactions between the elastomer and liquid medium are often accelerated at a higher temperature, thus severely degrading the materials. This temperature induced chemical degradation can introduce undesired crosslinks within the elastomer chain and contribute to a loss of elastomer flexibility.

Haseeb et al. (2010) studied the degradation of NBR and CR in biodiesel and reported that increasing the immersion temperature of the elastomer in biodiesel from room temperature to 50 °C could cause an increase in the mass of NBR. The mass gain occurred due to increased rate of absorption of biodiesel in NBR at a higher temperature. A similar trend was observed for CR. However, the increase in temperature caused less mass gain for CR as compared to that of NBR. Due to the polar nature of CR, it can then react with or dissolve in the polar components in biodiesel resulting in the gradual loss of mass. According to Haseeb et al. (2010), an increase in temperature also accelerates this phenomenon. It is important to note that the operating temperature (e.g. process liquid temperature) of any process is often known before hand and can be well controlled during the operation. Therefore, a suitable elastomer to withstand such a known range of temperatures can be selected easily to help prevent elastomer degradation in the process.

2.4.2 Elastomer Testing

As mentioned earlier, the selection of elastomers is practically based on compatibility tables obtained from elastomer suppliers. However, the tables are too simplistic to predict the resistance between the elastomers and the liquid mediums, which are usually complicated multi-components mixtures in actual chemical processes. Moreover, the degradation of elastomers becomes more complex in accordance with the development of more complicated elastomers and contacting media. Therefore, this has made the degradation of rubber to recently gain much interest in many fields of study. Various compatibility issues of elastomers in many automobile components can be complicated due to the difference between petro-diesel (i.e. mixture of hydrocarbons) and

biodiesel (mixture of methyl ester), and their compatibility with elastomers. Trakarnpruk and Porntangjitlikit (2008) studied the compatibility of six types of elastomers (i.e. NBR, HNBR, NBR/PVC, acrylic rubber, co-polymer FKM, and ter-polymer FKM) with 10% mixture of palm biodiesels in diesel. The results showed that only co-polymer FKM and ter-polymer FKM had good resistance to the solution, showing only a small change in their properties after immersion.

Haseeb and coworkers studied the compatibility of NBR, CR and fluoroviton A with mixtures of diesel and palm biodiesel. The results showed that fluoroviton A had high resistance to diesel and biodiesel mixtures. Later, Haseeb (2011) published another work focusing on the physical properties of some additional elastomers usually used as gaskets or o-rings in diesel fuel engine systems such as EPDM, SR, CR, PTFE, and NBR. The results showed that PTFE had the highest compatibility with biodiesel. Linhares (2012) studied the compatibilities of NBR with biodiesel produced from coconut and castor bean oil. The results showed that NBR could be deteriorated by biodiesel. However, the degradation resistance could be improved by increasing the percentage of acrylonitrile content.

Apart from biodiesel, various studies have also been carried out to study the compatibility of elastomers in other solvents to ensure safety when used in a wide variety of applications. Baah et al. (2000) studied the degradation of polysulfide elastomers (Thiokol A) in various organic solvents, namely, acetic, citric and propionic acid. The mass of the elastomers decreased in every experimental condition due to the dissolution of rubber into the solution or the leaching of loosing particles from poorly prepared rubber surface.

Baah and Baah (2001) studied the effect of acetaldehyde, acetic anhydride, and malic acid on NBR, neoprene, and NR. The results showed that the mass of rubber increased for all cases due to the absorption of the solvents into rubbers. Also, Georgoulis et al. (2005) studied the permeation of toluene and MEK in natural rubber, nitrile rubber, and polyvinyl alcohol (PVA) gloves. Only negligible permeation of the solvents through PVA was observed. Toluene permeated more through natural rubber, while MEK permeated more easily in nitrile rubber.

Tan et al. (2009) studied the chemical stability of EPDM in PEM environment using a mixture of 12 ppm H_2SO_4 and 1.8 ppm HF. The results showed that the main chain of EPDM was relatively stable showing no significant change. However, SiO_2 which was used as the filler for EPDM, was released to the environment during immersion (Tan et al., 2009).

2.5 Degradation of Elastomers

Currently, a number of novel elastomers have been synthesized with structures that are even more complex in order to improve durability and provide a variety of elastomers for use in various applications. Due to such complex structures of the elastomers, studies of the degradation mechanisms of these human-made materials have become more difficult. Parker (1974) has described the general causes of polymer degradation that might be used to explain the degradation behaviour of elastomers. These can be divided into two categories: degradation from energetic attack and degradation from chemical attack.

2.5.1 Energetic Degradation

Energetic degradation results from thermal, mechanical, and/or radiant energy being applied to the polymer materials.

2.5.1.1 Thermal Degradation

According to Parker (1974), thermal degradation occurs from depolymerisation or "unzipping" of the polymer, which is the phenomenon of breakdown of polymer chains due to the application of heat. The polymerization is a reversible reaction. In most cases, at low temperature, the forward rate of reaction is much higher than the backward rate of reaction. If heat is introduced and the temperature increase reaches a temperature that the rate of polymerization is equal to the rate of reverse reaction. This temperature is called the ceiling temperature. Above this temperature, polymerization stops and the rate of de-polymerization increases. The polymer will transform to a monomer or other components generated from side reactions.

2.5.1.2 Mechanical Degradation

The application of mechanical forces can contribute to polymer degradation where the polymer chains are torn apart. This leads to a decrease in the molecular weight of the polymer. During the breaking of the polymer chains, it is believed that free radicals will be produced. If oxygen is present in the process, the free radical will quickly combine with oxygen to form carbonyl compounds. On the other hand, if no oxygen is present, the free radical that occurred due to the introduction of mechanical forces will repolymerize. Ultrasonic energy is one cause of mechanical degradation. The ultrasonic wave leads to the vibration of the polymer chain which will cause a breakage in the polymer chain after a period of time (Allen, 1992). However, this degradation tends to occur with only long

chain polymers. Small chains are not likely to degrade under these conditions. The degradation by ultrasonic energy would be expected to have only a small influence on the polymer molecular weight (Parker, 1974).

2.5.1.3 Degradation from Radiant Energy

Radiant energy can excite the electrons in polymers to a higher potential energy level and cause bonds between atoms to break. Lehrle and Pattenden (1998) reported that after irradiation by gamma radiation from Co-60, polyisobutylene showed a large decrease of molecular weight due to chain scission (Lehrle & Pattenden, 1998). Similar results were obtained by Ito (2007) when EPDM, HNBR, and AFLAS were exposed to Co-60 gamma rays causing damage and alteration to physical properties such as tensile strength of the polymer.

2.5.2 Degradation of Elastomers From Chemical Attack

Although energetic degradation can damage elastomers, this case does not usually occur. In real applications, the damage from energetic degradation usually takes place after the chemical deterioration of elastomers. According to Schweitzer (2010), elastomers become weaker after a chemical attack, and deteriorate more easily when acted on by energetic forces. The chemical deterioration of elastomers occurs from the chemical reactions between the elastomers and the liquid medium or by the absorption of the liquid medium into the elastomers. The reactions grouped into the chemical attack category are oxidation, hydrolysis, biodegradation, and dissolution of elastomers (Parker, 1974).

2.5.2.1 Oxidation

Oxidation is one of the most common reactions that occur with polymer materials. These reactions take place in the presence of oxygen. Normally, the product of the oxidation of the hydrocarbon polymer is carbonyl groups such as hydroperoxide or ketone. The mechanisms of the polymer oxidation are complex and vary with the structure of the polymers. In the case of saturated hydrocarbon, the oxidation reaction does not cause bond scissoring in the absence of sunlight. Unlike the polymer with double bonds, scission of the polymer chain might occur and the oxidation might be faster than for the saturated hydrocarbon. In their study of thermal oxidation of styrene butadiene copolymer, Norman et al. (2004), showed that the thermal oxidation can cause the formation of new crosslinks in the polymer. Moreover, they also observed that when the temperature increased from 90 to 110 °C, the rate of thermal oxidation increased, based on the observation of the rate of increase in the carbonyl group (Allen et al., 2004).

2.5.2.2 Hydrolysis

Hydrolysis is a reaction resulting from hydrogen ion (H^+) or hydroxyl ion (OH^-) breaking down the polymer chains of elastomers. The degree of hydrolysis depends on temperature and type of contacting fluid (Parker, 1974). It should be noted that most of polymers produced by condensation polymerization usually having functional groups such as ester, amide, imide and carbonate, are susceptible to degradation by hydrolysis since they can be attacked by either acids or alkalis or both (Wright, 2001). Mitra et al. (2006) studied the degradation of EPDM in acid environment by exposing the elastomer to a solution of Chromium (Cr) and H_2SO_4. They discovered that the acid could attack the EPDM elastomer via the unsaturated bonds in its side chains.

2.5.2.3 Biological Degradation

Biological degradation of polymers is the consumption of the polymer by a microorganism to obtain lower molecular weight products or to transform the material to biomass, CO_2 and methane or sometimes hydrogen sulfide depending on the reaction pathway. The ability to degrade in biological environment depends on the structure of the polymer such as functional group stability, reactivity, hydrophylicity, and morphology. For example, a polymer with amorphous structure will degrade before a polymer with high crystalline fraction. Bacteria, fungi and algae are the most important organisms for degradation of polymer materials (Leja & Lewandowicz, 2010).

2.5.2.4 Dissolution of Elastomer

Unlike small molecules, for which the dissolution rate follows the diffusion laws, elastomers are composed of long molecular chains, and their dissolution phenomenon in liquid is more complicated. Pekcan and Ugur (2002), has described the dissolution of elastomers into liquid to occur in three steps as shown in Figure 2.1 (a) – (c). In the first step (a), the liquid penetrates into the elastomer. The penetration distance depends on the free volume of elastomers which is a function of the flexibility of the elastomer chains, backbone, side group and thermal history. In the second step (b), the relaxing elastomer chains form gel layers consisting of both solutions of molecules and of elastomer chains. In the last step (c), elastomer molecules separate from the bulk material into the solution as a result of the transfer of mass of the elastomers. To illustrate the dissolution degradation process, Baah et al. (2000) studied the degradation of polysulfide elastomers (Thiokol A) in various organic solvents including acetic, citric, and propionic acids. They

found that the mass of the elastomers decreased due to the dissolution of the rubbers into the solution.

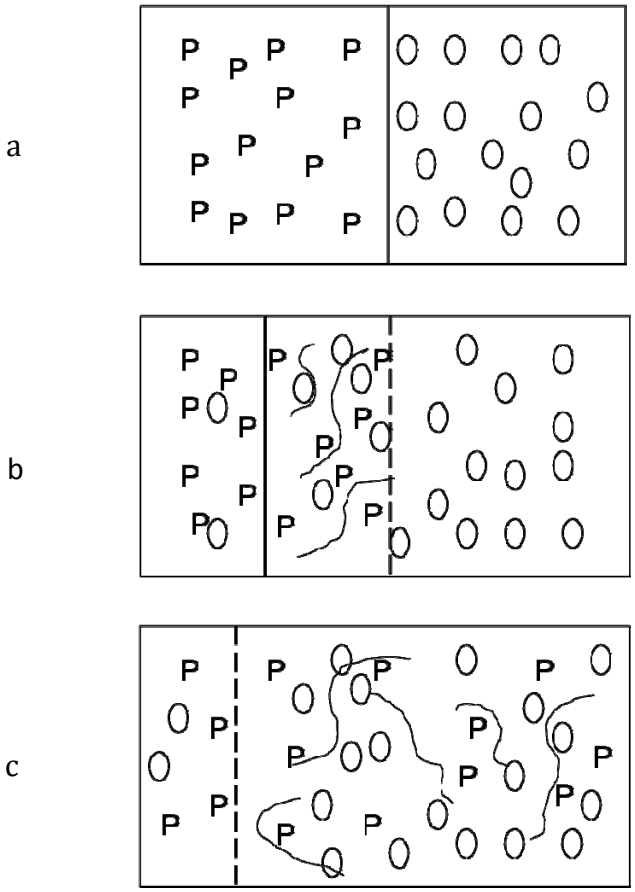

Figure 2.1 Mechanism of elastomer dissolution (Pekcan and Ugur, 2002)

(a) The penetration of solution into polymer

(b) The formation of gel layer

(c) The dissolution of polymer chain

2.6 Analytical Techniques for Determination of Elastomer Degradation

The results of the various pathways of degradation are changes in the chemical and physical properties of elastomers. The change of physical properties such as the decrease of molecular weight can affect some mechanical properties such as tensile strength, impact strength, and elongation at break. Moreover, changes in color can also result. Chemical changes can form undesirable functional groups and structures such as hydroxyl, carboxyl, unsaturated, and saturated structures. These changes can be investigated by several techniques.

2.6.1 Attenuated Total Reflectance Fourier Transform Infrared (ATR-FTIR)

FTIR is a powerful spectroscopic technique used in elastomer fields to identify functional groups of organic molecules. The principle of FTIR is that each molecule absorbs infrared light at a different frequency depending on the energy of molecular vibrations. Conventional FTIR technique requires sample preparation either in the form of liquid film, potassium bromide (KBr) pellet or thin film, in order to allow the infrared light to pass through the sample (Conley, 1972). Gunasekaran et al. (2007) utilized FTIR by using the liquid film method. The elastomer samples were cut in small pieces and melted. A drop of the melted material was smeared in sodium chloride (NaCl) disks that were used as a window in the liquid film technique. However, this technique could chemically alter the polymer structure due to the use of heat. To overcome this difficulty, ATR-FTIR has been utilized. ATR-FITR is an internal reflection technique introduced in the 1960s (ref). One of the strongest advantages of the ATR-FTIR technique is that it does not require sample preparation. The spectra is collected directly from elastomer

samples without sacrificing the sample (Do, Celina, & Fredericks, 2002). Nakamura et al. (2011) used the ATR-FTIR technique to obtain FTIR spectra of EPDM and found that carbonyl group occurred within the structure of EPDM used in water supply systems.

2.6.2 Scanning Electron Microscope (SEM)

SEM can be used to inspect the deterioration of material surfaces due to chemical attack. Haseeb utilized SEM to investigate some elastomer surfaces after exposure to a mixture of diesel and biodiesel. This investigation revealed pits and cracks on the elastomers surface as a result of the exposure to various diesel formulations (Haseeb et al., 2010).

2.6.3 Physical Property Measurement of Elastomers

The physical properties of elastomers considered in this thesis are tensile strength and hardness. Tensile strength is measured to ensure rubber compound uniformity to indicate the deterioration of rubber after contacting with liquid medium.

Tensile strength, presented in terms of ultimate elongation, was used by Ito (2007 to study the degradation of elastomers (i.e. EPDM, HNBR, AFLAS) by heat and radiation. After the elastomers were exposed to Co-60 γ-ray at 70 °C, the ultimate elongation of the elastomers decreased. This is because the high energy of radiation and the electrons generated in the elastomers due to the radiation cut the main polymer chain (Ito, 2007).

Typically, hardness is defined as the resistance to indentation. Due to differences in chemical structure, each elastomer has its own inherent hardness. Polymer material

hardness can be measured in two ways. The Rockwell method is suitable for rigid material such as hard plastic while the Durometer method is used to measure hardness for softer materials such as elastomers. The scale of the Durometer is varied from 0 to 100 indicating the range of hardness of a material from low to high. Trakarnpruk and Porntangjitlikit (2008) measured tensile strength and hardness of elastomers (i.e. NBR, HNBR, NBR PVC, Acrylic rubber, Co FKM, and Ter FKM) to show the results of the deterioration from immersion in biodiesel. The results showed a highly decreasing trend of hardness of high swelling tendency rubbers like Acrylic and HNBR after immersion, compared to the others elastomers. However, tensile strength was not affected as its change was not significant.

CHAPTER III

EXPERIMENTS

3.1 Elastomers, Chemicals and Equipment

The raw elastomers used in this study were EPDM, SBR, NR and IIR. There were obtained from MDR International Co., Ltd., Bangkok, Thailand. The commercial elastomers tested were commercial EPDM, IIR and PTFE. There were in the form of sheets with thickness of 1.57 mm and were purchased from Rubber Sheet Roll, Pennsylvania, USA.

Aqueous MEA (of molarities of 3, 5 and 7 M) as well CO_2-loaded aqueous MEA (with 5 M MEA with loadings of 0.16, 0.25, 0.5 mol CO_2/mol MEA) solutions were prepared from laboratory grade MEA purchased from Fisher Scientific, Ontario, Canada. Research grade 100% CO_2 used for the CO_2-loaded experiments was supplied by PRAXAIR, Canada. Hydrochloric acid with the concentration of 1 normal was purchased from VWR, USA which, along with 0.1 % methyl orange solution (obtained from Sigma-Aldrich, Canada) was used in the titration to determine the CO_2 loading. Potassium phosphate monobasic (KH_2PO_4) and phosphoric acid (H_3PO_4) solution reagent grade purchased from Sigma-Aldrich, Canada were used for the mobile phase of High Performance Liquid Chromatography **(**HPLC).

A 600 mL stainless steel batch reactor model 5500 (Parr Instrument Co., Moline, IL) equipped with a programmable temperature controller model 4836 with a tachometer display module (Parr Instrument Company, IL, USA) was utilized in high temperature commercial elastomer testing. ATR-FTIR spectra of elastomer samples were recorded

from Nicolet iS5 with diamond crystal (Thermo Fisher Scientific Inc., Canada). SEM model JSM-5600 (JEOL USA Inc., Peabody, MA, USA) was used to capture the images of the elastomer surfaces. The sputter coater used was model Quorum CC7650R SEM Carbon Coater (Soquelec Ltd., Quebec, Canada), which is designed to coat up to six SEM samples at one time. The carbon rods 6.15 mm diameter and 100 mm (unshaped) were purchased from Soquelec Ltd. The Nuclear Magnetic Resonance **(**NMR) used for analysis of elastomer gel was a model Agilent/Varian MercuryPlus 300M Hz with an ATB (Automation Triple Resonance Broadband) probe. The HPLC used for analysis of the liquid samples was equipped with refractive index detector (RID), Diode Array detector (DAD) and an on-line degasser (model 1100/G1362A/G1315B, Agilent Technologies Canada, Mississauga, Ontario, Canada). The column used was Nucleosil 100-5 SA containing a strong cationic exchanger of sulphonic acid (Macherey-Nagel, Germany) of 250 mm in length and 4.6 mm in diameter. The samples were introduced to HPLC automatically by an auto-sampler (model G1313A Agilent Technologies Canada, Mississauga, Ontario, Canada). Density and viscosity of the solutions were measured using 2000 ME Microviscometer (Anton Paar, Graz, Australia) equipped with density meter (DMA 4100/4500/5000 M), viscosity meter (DSA 5000 M) and an automatic sample changer (Xsample). The refractive index of the solutions was measured with Abbemat 550 (Anton Paar, Graz, Australia).

3.2 Screening of Elastomers

The initial screening of the elastomers was performed by collecting compatibility tables from elastomer suppliers. The compatibility tables rate elastomeric materials in

contact with various chemicals by considering the results of static immersions in pure or aqueous solutions in small ranges of temperature. The compatibilities of elastomers with common amine solvents used for CO_2 capture processes including MEA, DEA and Triethanolamine (TEA) are accessible, and the list is shown in Table 3.1. Even though the companies do not provide the elastomer compatibility data at the exact CO_2 absorption operating condition, this data provides good guidance in the selection of elastomers.

From Table 3.1, it can be seen that the most recommended elastomers for MEA are Ethylene Propylene Diene Monomers (EPDM), Isobutylene Isoprene Rubber (IIR), Styrene Butadiene Rubber (SBR), Natural Rubber (NR), and Isoprene Rubber (IR). As the chemical structures of IIR and IR are very similar, four types of elastomers – EPDM, IIR, SBR, and NR – were selected for further tests.

Table 3.1 Compatibility data of elastomers and amine used in CO_2 absorption

Chemicals	FKM	HNBR	FVMQ	EPDM	NBR	CR	ACM	ECO	AEM	CSM	IIR	SBR	NR	IR	AU	T	Source
DEA					2	1				3	1	2		2			PPE Limited
	3		1	1	3	1	4			1	1	1			4		MYKIN INC.
	3	3	1	1	3	1					1	1	1		4		Macro rubber
MEA	4	4	4	2	4	4	4	4	4	4	2	2		2			PPE Limited
			4	1	4	4	4			4	2	2	2	2	4	4	DUPONT
	4		4	2	4	4	4			4	2	2			4		MYKIN INC.
	4		4	2	3	4				4	2	2	2		4		Mid Atlantic Rubber CO.
	4	2	4	2	4	2	4				2	2	2		3		Macro rubber
TEA	3	3	3	2	3	2	4	3	3	3	2	2		2			PPE Limited
		3	4	2	3	4	4	2	1	2	2	2	2	2	4	4	RLHUDSON
		3	4	1	2	1	4		2	2	2		2	2	4	4	DUPONT
	4		4	2	3	1				1	2	2	2		4		Mid Atlantic Rubber CO.
	4			2	3												PSP INC.
	4	3	4	2	3	2	4				2	2	4		4		Macro rubber

(1 = Excellent, 2 = good, 3 = doubtful, 4 = not recommended)

3.3 Solvent Preparation

The solvents used in the experiments were 3, 5, and 7 M MEA aqueous solutions and 5 M MEA with loading of CO_2 varied from lean to rich (0.16, 0.25, and 0.5 mol CO_2/mol MEA). The solutions were prepared by dilution of MEA with deionized water. The concentrations then were checked for accuracy by titration with standard solution of 1 M hydrochloric acid (HCl). Methyl orange with the concentration of 0.1wt% was used as an indicator. For MEA solutions with CO_2 loading, the MEA solutions were first prepared to the desired concentrations and then purged with 100% CO_2. CO_2 loading (mol CO_2/mol MEA) was measured following the standard procedure provided by the Association of Official Analytical Chemists (AOAC) (Horwaitz, 1975). The concept of this method was basically an acidification technique where the CO_2 loading was determined from the titration-based calculation. The MEA concentration can be measured directly from the titration of the solution with 1 M HCl. During titration, HCl reacts with MEA to reverse CO_2-MEA reactions and desorb the CO_2 from solution. After the end point of titration, excess 1 M HCl was added into the loaded solution to ensure that all CO_2 was released. The amount of CO_2 dissolved in the solutions was calculated from the released gas collected in a precision burette containing displacement solution of NaCl/$NaHCO_3$/methyl orange mixture. Finally, the CO_2 loading was calculated as a ratio of mole of CO_2 released from the solution and moles of MEA in the samples.

3.4 Preliminary Screen Test of Raw Elastomers

This test was conducted to screen the selected elastomers (EPDM, SBR, NR and IIR) in their raw stages, identified as unfinished rubbers, containing no fillers and

additives, in order to test their chemical resistance. Raw elastomers were tested as the resistance to chemicals of seal and gasket materials depends mainly on their base polymers, while the additives or fillers are responsible for improvement of their physical properties (Schweitzer, 2010).

3.4.1 Sample Preparation

The method of elastomer immersion in MEA solution was adapted from ASTM D417-10. The standard test method for rubber property-effect of liquid was employed for this test. Since the raw elastomers received from the suppliers were mostly non-uniform, cutting the samples into the exact dimension indicated in the ASTM D471 proved to be difficult and unnecessary. Therefore, the samples were first cut approximately into rectangular shape of dimension 2x25x50 mm. Then the size of each specimen was adjusted to give a weight of 2 g.

3.4.2 Immersion of Raw Elastomers

The elastomers selected from the previous section were tested in 3, 5 and 7 M MEA aqueous solutions and 5 M MEA solution with loading of CO_2 from 0.16, 0.25, 0.50 mol CO_2/mol MEA which is typical of conditions in CO_2 absorption processes. For a preliminary test, the four selected raw elastomers were first immersed at the low temperature of 40 °C, which is typical of absorber temperatures in CO_2 absorption processes. The immersion of the specimens was carried out in test cells with dimensions of 12 inches long and 1.5 inches diameter. Each tube contained 100 mL of the desired concentration of aqueous MEA solution where 3 specimens of known weight were

immersed. The three specimens were suspended by a stainless steel wire, and each piece was separated from the others by 0.6 mm diameter perforated glass beads as shown in Figure 3.1. A rubber stopper served as the lid to the test cell and was used to suspend the wire so that the specimens were kept steadily immersed in the solution throughout the test. A water bath capable of controlling temperature within 0.5 °C was used to control the temperature of the MEA and test specimens at 40 °C. A reference test cell without any test specimens containing only MEA solution similar to that used in the sample test cells was also kept under the same test condition. During the immersion, the possibility that degradation products of MEA and CO_2 might be generated in the solution required the reference cell to serve the purpose of distinguishing between dissolution components from elastomers or degradation products of MEA solutions themselves.

After 30 days of immersion, both the elastomer samples and the solutions were analyzed. The elastomers were first rinsed in deionized water and dried at room temperature according to procedures reported in the literatures (Wang et al., 2004Mosadegh-Sedghi et al., 2012; Sedghi et al., 2011). The samples were weighed every 24 hours until constant weight was achieved. The constant weight was taken as weight of elastomers after the immersion and the mass change of the elastomers was calculated. On average it took 2 days for a sample to reach a constant weight. Moreover, the elastomer samples were taken for analysis of chemical structure by FTIR. The solutions were analyzed by HPLC, and physical properties, namely, density, viscosity and refractive index were measured. The results of the solution analysis obtained from cells with elastomers were compared with those from the reference cells.

3.5 Commercial Elastomer Testing

After the preliminary testing of the raw elastomers, two elastomers, namely EPDM, IIR and PTFE were selected for testing in their commercial form. PTFE was added in the commercial material testing step due to its well known high chemical resistance as a result of its saturated and fully fluorinated backbone. PTFE is widely used for sealing and piping application. Therefore, it is apparent that its raw state has excellent resistance to a wide range of chemicals including MEA. These three elastomers were tested for their physical properties to ensure their suitability for use in CO_2 absorption with MEA processes.

3.5.1 Sample Preparation

As the elastomers tensile strength would be measured to investigate the physical property changes, the samples were prepared in dumbbell shapes following the ASTM D412, Standard Test Methods for Vulcanized Rubber and Thermoplastic Elastomers – Tension. The shape and dimension of dumbbell Die C cutting can be found in the ASTM D412. Before starting the experiments, the weight of each specimen was measured and recorded.

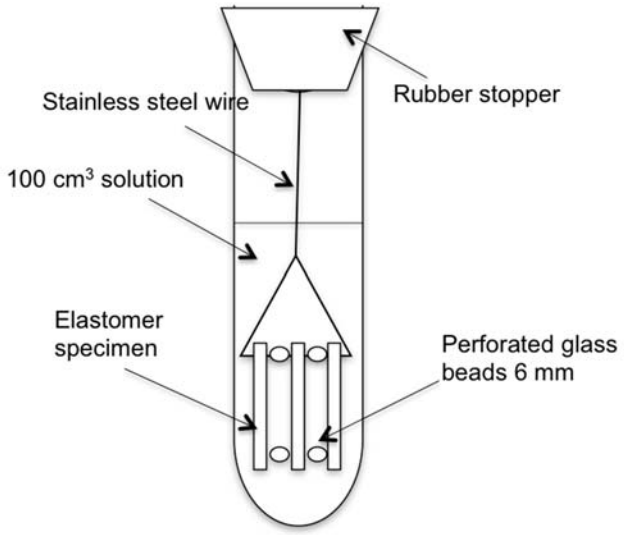

Figure 3.1 Immersion cell diagram

3.5.2 Immersion of Commercial Elastomers

The commercial elastomers EPDM, IIR and PTFE were tested in a solution of 5 M MEA with 0.5 mol CO_2/mol MEA at the temperature of 40 and 120 °C. For the tests at the temperature of 40 °C, which is the temperature typically used in the absorber, the immersion was carried out in glass test tubes as mentioned earlier in raw elastomer testing section. Three pieces of specimens and 120 mL of the solutions were loaded into the glass test tubes. The test tubes were put in the water bath to control the temperature at 40 °C.

The temperature of 120 °C, which is the temperature used in the CO_2 stripping section of the process, was used for the tests. The apparatus and procedure used for the raw elastomer testing is not suitable at 120 °C; therefore, the immersion test of the commercial elastomers was carried out in a batch autoclave reactor. This served to ensure that the compositions of the solutions remained constant during the test. The images of a fully equipped reactor and a reactor head are presented in Figures 3.2 and 3.3, respectively. The reactor was also equipped with a magnetic drive stirrer with a variable speed motor at 1.17 hp and an aluminum block heater with a heat power of 1000 watts, which required an electrical supply of 115 volts. For each run, the three dumbbell specimens of known weight and 450 mL of the solutions were loaded into the reactor. Due to the reactor being full with the accessories from the reactor head, the specimens were hung on a stainless steel wire attached to the stirrer blade which was moved up close to the top end. It should be noted that there was no stirring throughout the duration of the immersion test. The loaded reactor was assembled into a block heater, attached to a temperature controller by plugging in the thermocouple, connecting the cooling solution

(50%wt ethylene glycol in water) through the cooling loop, and ensuring closure of all valves. The experimental temperature was set at 120 °C and kept constant for the 30 days of immersion. At the end of the immersion period, the temperature controller was assigned to cool down the solvents and the specimens to 25 °C. Then, the specimens were removed from the reactor.

After 30 days of the immersions, each specimen was quickly dipped in acetone and blotted lightly with filter paper free of foreign material as in ASTM D471. The weights of each specimen were measured with a four decimal weight scale. Three pieces of the specimen were sent for testing for the physical properties of tensile strength and hardness. Another piece of the specimen was tested for surface degradation with SEM.

Figure 3.2 A fully equipped reactor (Original in color)

(Wattanaphan, 2012)

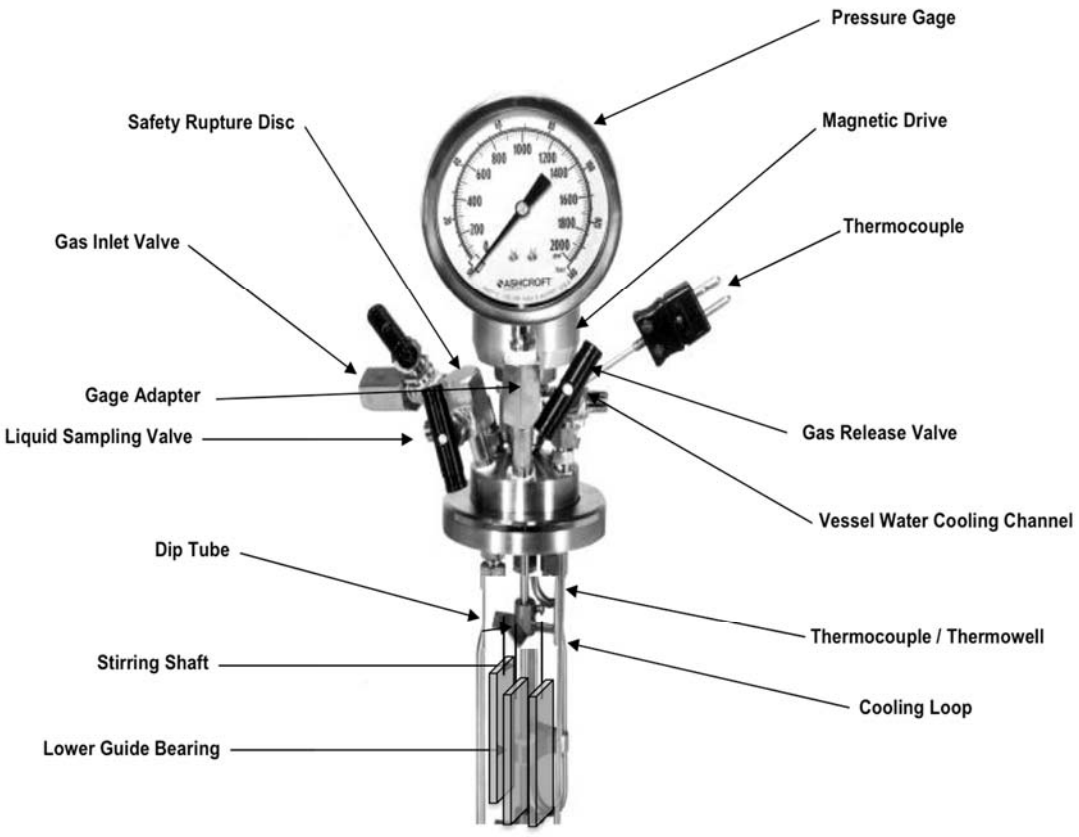

Figure 3.3 Reactor head with elastomer specimens

3.6 Elastomer Analysis

Degradation of the elastomer samples was assessed using the measurement of mass change, Attenuated Total Reflectance-Fourier Transform Infrared Spectroscopy (ATR-FTIR), Scanning Electron Microscopy (SEM), as well as tensile strength and hardness tests.

3.6.1 Mass Change of Rubber

The mass change of the elastomers was calculated by using the equation written in ASTM D471 as in the following:

$$\% \Delta M = \frac{(M_2 - M_1)}{M_1} \times 100 \qquad (3.1)$$

where %ΔM, M_1 (g), and M_2 (g) are the percentage of mass change, the mass of specimen before immersion and the mass of specimen after immersion, respectively.

3.6.2 Attenuated Total Reflectance Fourier Transform Infrared (ATR-FTIR)

To investigate the chemical change in the elastomers after the immersion in the solutions, the ATR-FTIR technique, which has ability to identify functional groups of organic and inorganic compounds, was utilized. With the ATR technique, the infrared spectroscopic analysis can be carried out with no requirement for sample preparation. The elastomer specimens were placed on the ATR diamond crystal; then, a pressure arm was rolled down to ensure good contact between the elastomer specimens and the diamond crystal. All IR spectra were recorded at room temperature in the range of wave number of 550 to 4000 cm^{-1}. The resolution and the number of scans were 6 cm^{-1} and 32, respectively.

3.6.3 Scanning Electron Microscopy (SEM)

Elastomer samples were prepared in sample stubs and coated with carbon. After coating with carbon, the samples were placed into the SEM analysis chamber. For each sample, images at 100x, 250x, 500x, and 1000x magnifications were collected at 20kV energy level. The capturing of images was done as fast as possible to prevent sample charging.

3.6.4 Tensile Strength and Hardness Testing

The commercial elastomers specimens were sent to The Industrial Technology Centre (Manitoba, Canada) to measure their tensile strength and hardness. The tensile tests were performed under the ASTM D412. The hardness of the specimens was obtained using a Durometer with a presser foot of type A.

3.7 Liquid Analysis

3.7.1 High Performance Liquid Chromatography (HPLC)

The mobile phase used was 0.05 M potassium hydrogen phosphate adjusted to a pH of 2.6 by adding 85% w/w KH_2PO_4. The mobile phase was degased for at least 3 hours in an ultrasonic bath follow by filtration with 0.20 μm nylon membrane filter. The mobile phase was fed with isocratic method with 100% of a single mobile phase at a flow rate of 1.0 mL/min. The column temperature was kept at 35 °C for all analyses. The method was based on the work of Supap (2007) and Wattanaphan (2012) which aimed to study the degradation products of MEA during CO_2 capture process. The samples were diluted to 1:100 and filtered through 0.20 μm nylon membrane filters. The samples were

introduced to HPLC automatically by an auto-sampler with an injection volume of 20 μL. Nanopure water was used for the mobile phase preparation and the sample dilution. As mentioned above, two detectors equipped with HPLC were used. RID was used mainly for analysis of MEA concentration because of its limitation in the detection of diluted samples. Chromatograms obtained from DAD were particularly examined for low concentration products such as dissolved components from elastomers. Moreover, 10 ppm of imidazole was added into some samples as a reference peak for cases where relative concentration was studied.

3.7.2 Nuclear Magnetic Resonance (NMR)

NMR was used to analyze the dissolved elastomer compounds that were in the solid form. The solid compounds were first separated from the solutions by centrifugation. The separation process resulted into two phases of the solution. The top phase was a solid gel layer while the bottom phase was the aqueous solution of MEA. The top solid gel layer was taken out and mixed with $CDCl_3$ as a solvent for the NMR test performed at 27 °C.

3.7.3 Physical Properties of the Solutions

Before measuring physical properties, the solutions from both the reference cells and the cells with immersed elastomers were filtered with a 0.20 μm nylon membrane filter. Approximately, 10 mL of the solutions were used to fill the capillary tubes. The capillary tubes were inserted into the automatic sample changer to measure density and viscosity. The following steps were taken for refractive index measurements: two or three

drops of filtered samples were dropped into the refractometer sample cell, the lid was applied to cover the solution, and then the the measurement was started. After measuring the refractive index, the cell was cleaned with acetone before starting the next measurement. All the physical properties of the solutions were measured at 25 ^{o}C.

$$\% \Delta X = \frac{(X_{cell} - X_{ref})}{X_{ref}} \times 100 \quad (3.2)$$

where %ΔX, X_{cell}, and X_{ref} are the percentage of physical properties change, the physical properties from the cell with elastomers the physical properties from the reference cells, respectively.

CHAPTER IV

RESULTS AND DISCUSSIONS

4.1 Raw Elastomer Testing

4.1.1 Physical Appearance of Raw Elastomers

The raw elastomer specimens (IIR, EPDM, SBR and NR) were immersed in solutions of 3, 5, 7 M as well as 5 M MEA loaded with 0.16, 0.25 and 0.5 mol CO_2/mol MEA) for 30 days at 40 °C. The results obtained were compared with those of the corresponding original specimens as shown in Figure 4.1. The comparison between the original IIR specimen and immersed IIR specimens is presented in Figure 4.1 (a). It shows that IIR stretched during immersion in both aqueous MEA and aqueous MEA/CO_2 solutions. The stretching of the specimens could have occurred due to the force of gravity as they were suspended on stainless steel wires. There were no other differences between the specimens after exposure to the solutions of MEA and MEA/CO_2.

For the EPDM specimens shown in Figure 4.1 (b), the original EPDM specimen and the specimens after immersion in MEA and MEA/CO_2 looked very similar; however, yellow spots were observed on the specimens after the immersion, especially at higher concentrations of MEA. These spots are suspected to be the MEA that remained even after the washing step. As all the specimens were washed with the same washing procedure, the samples immersed in higher concentration of MEA are more likely to have retained more MEA. Also, there was no significant difference of appearance between the specimens exposed to 5 M MEA and the 5 M MEA loaded with CO_2.

For the SBR samples in Figure 4.1 (c), the color of the original specimen is light yellow. After the immersion, the color of the SBR specimens changed to dark yellow. The yellowness of the polymer can be attributed to the presence of the ketone group which is usually the product of oxidation of the polymer (Parker, 1974) or the absorbed MEA in the elastomer specimens. The specimens exposed to MEA and MEA/CO_2 solutions had almost the same appearance.

The effect of immersion on NR is shown in Figure 4.1 (d). The differences between the original specimen, the specimens immersed in MEA solution, and the specimens immersed in CO_2-loaded MEA solutions can be easily distinguished in this elastomer. Beginning with the comparison between the NR specimens in their original state and the specimens after immersion in MEA solutions (3, 5, 7 M), the specimens exposed to the solutions were swollen at all the experimental concentrations; however, it was not easy to physically distinguish the effect of MEA concentration on the degree of swelling. The swelling of NR was likely due to the result of the absorption of the solutions or the occurrence of chemical reactions between NR and the solutions. In contrast, the specimens that were exposed to the solution of MEA/CO_2 (5 M MEA with 0.16, 0.25 and 0.5 mol CO_2/mol MEA) gave a different result. The NR specimens did not swell with the addition of CO_2 in the solution. This is because CO_2 and MEA aqueous solutions formed some complex components, which made it difficult for the solution to penetrate the NR to cause swelling.

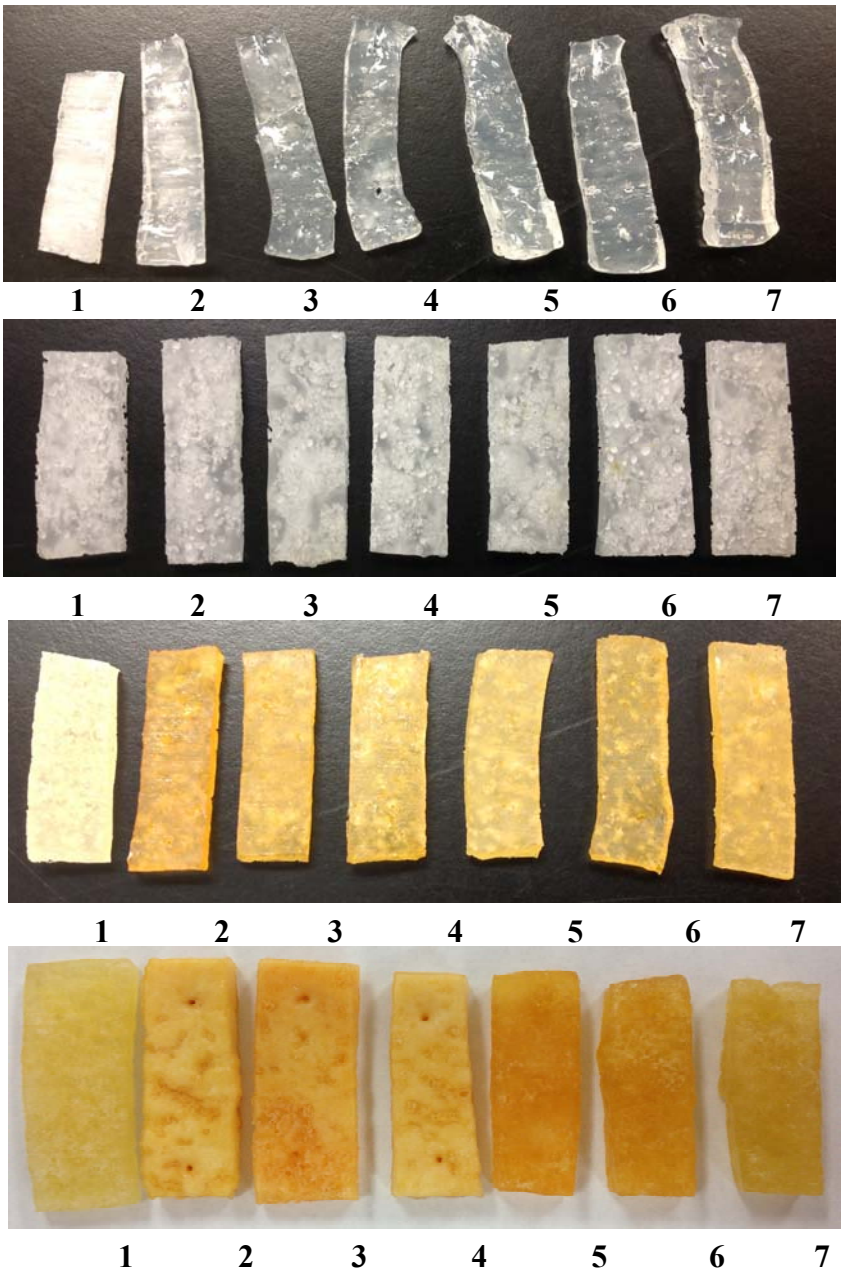

Figure 4.1 The raw elastomers of (a) IIR, (b) EPDM, (c) SBR, (d) NR

(Experimental condition: 30 days of immersion, 40°C)

Number 1 is specimen before immersion.

Number 2, 3, 4 are specimens after immersion in MEA 3, 5, 7 M.

Number 5, 6, 7 are specimens after immersion in MEA 5 M with 0.16, 0.25 and 0.5 mol CO_2/mol MEA.

4.1.2 Mass Change of Raw Elastomers

The mass change of elastomer is one of the parameters that can be used to indicate the compatibility between elastomers and liquids. The incompatibility of elastomer and liquid medium can result in either a decrease or an increase in mass. The adsorption or chemical reaction to form new compounds on elastomer surfaces causes increased mass, while the dissolution of elastomers contributes to a loss in mass. These phenomena can occur simultaneously. Therefore, the measured mass is the net mass of elastomers. The percentage mass change of the elastomers (IIR, EPDM, SBR and NR) after the immersions for 30 days at 40°C was calculated following the equation in ASTM D412 and were plotted against MEA concentration (3, 5, 7 M) and CO_2 loading (0.16, 0.25, 0.5 mol CO_2/mol MEA in 5 M MEA). The results obtained are shown in Figure 4.2 and Figure 4.3, respectively.

The results from Figure 4.2 displaying the effect of MEA concentration on the percentage mass change of the elastomers (IIR, EPDM, SBR and NR) after being immersed in the MEA solutions (3, 5, 7 M) for 30 days at 40°C shows that the percentage mass change of the elastomers was positive at every MEA concentration, implying that the mass of the elastomers increased in every case during immersion. NR had the highest percentage mass change compared to the other elastomers. This was followed by SBR, EPDM and IIR in that order.

The increase in the mass of NR immersed in the MEA solutions was also seen clearly in the physical observation section, as the NR specimens were swollen after immersion. NR is a homopolymer of cis-1,4-polyisoprene. The structure of the polymer has a low level of interlocking between the polymer chains resulting in high permeability

of gas and liquid (Chandrasekaran, 2009). Moreover, the double bonds in the isoprene structure leads to chemical instability (Chaikumpollert et al., 2011; Ciesielski, 1999). For the two reasons of high permeability of gas and liquid, and low chemical stability, NR was likely to interact with MEA by physical or by chemical adsorption resulting in an increase in mass. No definite trend was observed between MEA concentration and the percentage mass change of NR. This might be because some of the NR specimens were slightly porous. Besides, the porosity of all the specimens was neither the same nor uniform. According to Baah et al. (2000), since the total surface area of elastomer specimens exposed to liquid depends on these pores, comparing the mass change of specimens with different porosity might lead to inaccurate results.

SBR was another elastomer with a high content of double bonds in its elastomer chain. The mass of the SBR specimens increased during their immersion (in 3, 5, 7 M MEA), and the percentage of mass change increased with increasing MEA concentration. From physical appearance, it was observed earlier that the samples became more yellow after the immersion of SBR in MEA solutions. Therefore, the increase in mass and the change in color are a result of the physical and/or chemical absorption of MEA into the SBR specimens. It is possible that MEA chemically reacted with the double bonds in the SBR elastomer chain due to their high chemical reactivity.

The percentage mass change for EPDM increased with MEA concentration (3, 5 and 7 M). This was similar to the results for SBR. However, the percentage mass change is very small in this case. As the backbone of EPDM contains mainly the monomers of ethylene and propylene which is saturated and highly chemically stable (Tan et al., 2009), the chance of EPDM reacting with MEA is very low. The increase of mass of EPDM was

likely due to the remaining MEA on the surface as seen in the form of the yellow spots, as mentioned earlier.

IIR is the only elastomer in the experiment that had no mass change during immersion (in 3, 5 and 7 M MEA). IIR is a polymer with a high content of isobutylene and a small amount of isoprene (i.e. approximately 3%), (Dong et al., 2010). The methyl groups present in isobutylene monomer act as an interlock in the polymer chain, giving IIR its outstanding low permeability of gas and liquid (Chandrasekaran, 2009). This made it difficult for MEA to be adsorbed into the IIR elastomer, and reduced the chances of any reactions taking place.

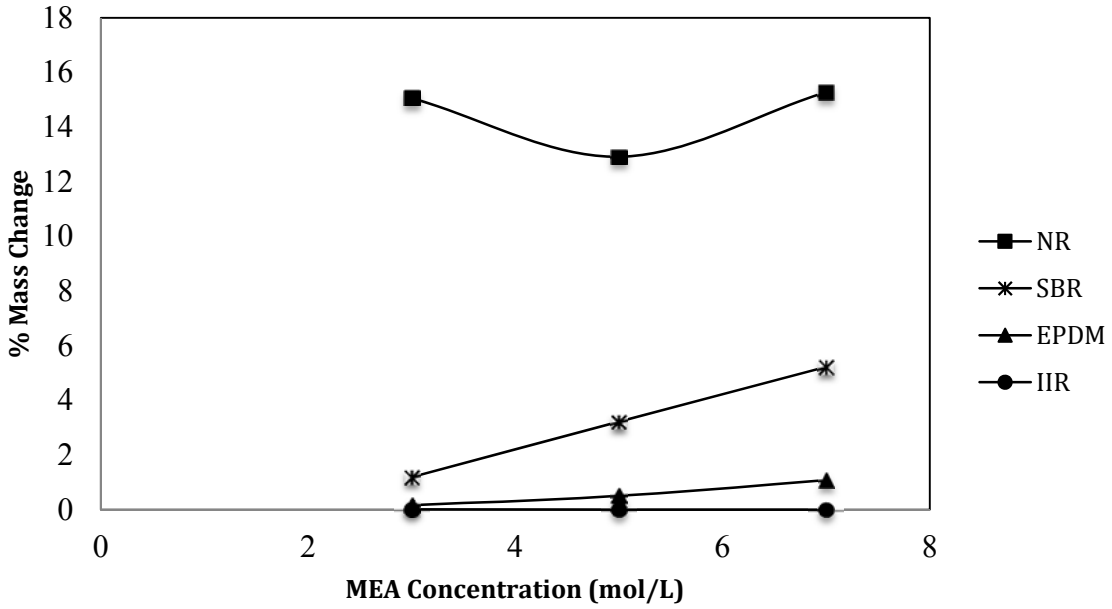

Figure 4.2 Effect of MEA concentration (3, 5, 7 M) on the percentage mass change of elastomers (IIR, EPDM, SBR, and NR)

(Experimental condition: 30 days of immersion, 40°C)

Figure 4.3 reveals the effect of CO_2 loading (0.16, 0.25 and 0.5 mol CO_2/mol MEA in 5 M MEA) on the percentage mass change of the elastomers (IIR, EPDM, SBR and NR). The result shows that increasing the CO_2 loading led to a reduction in percentage mass change of NR. This trend agreed with the result in section 4.1 (Physical Appearance) that found NR to be less swollen in the MEA/CO_2 solutions than the unloaded MEA solutions. In MEA/CO_2 solutions, MEA and CO_2 typically interact to form a complex electrolyte system containing mainly free MEA, carbamate, protonated MEA, and a small amount of bicarbonate and carbonate ions. The concentration of these components is a function of CO_2 loading (Sedghi et al., 2011). The ion species in the solution contributes to an increase in solvent polarity. According to Georgoulis et al. (2005), NR as a non polar elastomer is more swollen in non polar solvents than in polar solvent (Georgoulis et al., 2005). Therefore, the dissolved CO_2 that contributed to the higher polarity of the solution decreased the swelling of NR. In addition, the increase in CO_2 loading increased the surface tension of the MEA solutions. Normally, the surface tension of MEA solutions is lower than that of water. Thus, the solutions become better able to penetrate into the elastomer pores. However, the dissolution of CO_2 into MEA solutions increased the surface tension of the solutions as the polarity of the solution was increased (Sedghi et al., 2011). Similar results occurred with DEA solution as mentioned by Wang et al. (2004). The higher surface tension of CO_2 loaded amine solutions leads to a lower tendency to spread on materials compared to the aqueous amines. This made NR to be less swollen in solutions with higher CO_2 loadings.

SBR is the only elastomer for which the percentage mass change was found to be negative after immersion in the MEA/CO_2 solutions (0.16, 0.25 and 0.5 mol CO_2/mol MEA in 5 M MEA). Moreover, the percentage loss of mass became more pronounced with increasing CO_2 loading. In other words, increased CO_2 loading led to a higher loss of SBR mass into the solutions. This might be because CO_2 acted as an oxidant (Raju, Reddy, & Park, 2012). According to Williams (1937), the oxidation of elastomers contributes to chain scissoring and dissolution of the elastomer into the solution. Moreover, the higher CO_2 loading of MEA solutions increased the degree of oxidation and contributed to more solvation of the SBR.

Whereas increasing the MEA concentration had a positive effect on the percentage mass change for EPDM, the CO_2 loaded into aqueous MEA did not have any significant effect. The percentage mass change of EPDM is very low and almost constant with the variation in CO_2 loading. In this case, the solution of 5 M MEA without CO_2 as well as the one with CO_2 loading from 0.16 to 0.5 mol CO_2/mol MEA, resulted in mass changes of EPDM that were very similar. The slight increase in mass of the EPDM samples might come from the residual solutions on the elastomers.

In the case of IIR, the percentage mass change is close to zero and can be regarded as negligible at every CO_2 loading in 5 M MEA. This is due to the high stability due to the presence of non-polar saturated elastomer backbones. Moreover, the side chains of the elastomer help to prevent the permeation of the solution into the elastomer (Chandrasekaran, 2009). Therefore, the mass of the IIR specimens did not change after the immersion in MEA and MEA/CO_2 solutions.

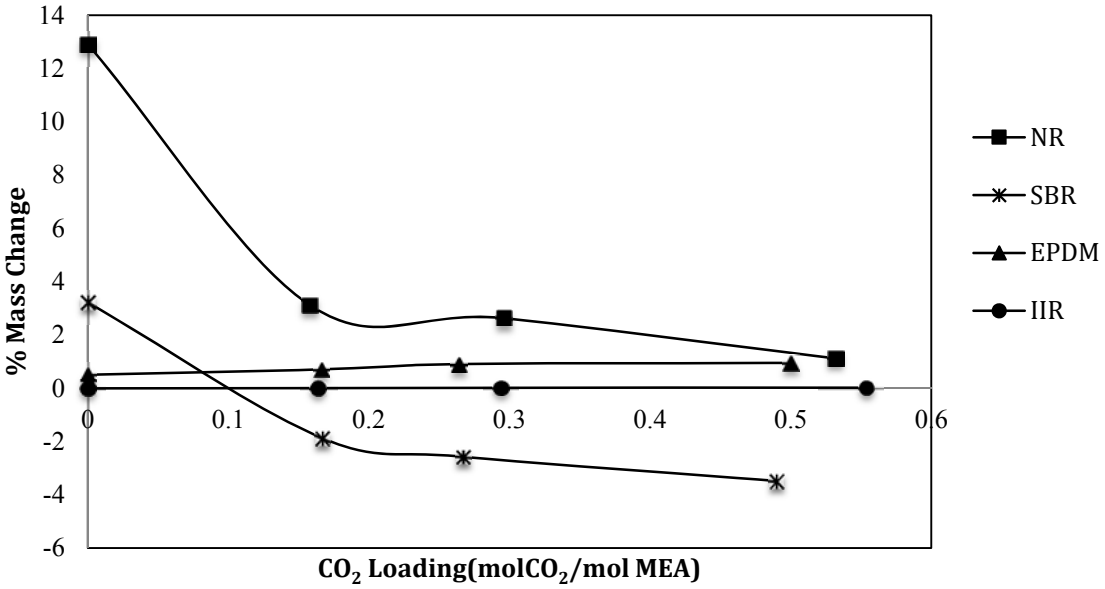

Figure 4.3 Effect of CO_2 loading (0.16, 0.25 and 0.5 molCO_2/molMEA in 5 M MEA) on the percentage of mass change of elastomers (IIR, EPDM, SBR, and NR) (Experimental condition: 30 days of immersion, 40°C)

In summary, the results from the percentage mass change of the elastomers show that IIR and EPDM are more likely to withstand both MEA and MEA/CO_2 solutions as they experienced very small changes in mass during immersion. On the other hand, both SBR and NR were highly swollen in the MEA solutions because of MEA adsorption and/or the chemical reactions that occurred. In MEA/CO_2 solutions, the swelling of NR decreased with increasing concentration of CO_2 but was still higher than those of IIR and EPDM. For SBR, increasing CO_2 in solution led to a loss of mass.

4.1.3 Chemical Structure Change of Elastomer

During immersion, there was potential for chemical reactions between the elastomers (IIR, EPDM, SBR and NR) and the solutions (3, 5 and 7 M MEA as well as 5 M MEA with 0.16, 0.25 and 0.5 mol CO_2/mol MEA) that would bring about chemical changes such as the formation of new functional groups in the elastomers. FTIR spectra were obtained using the ATR technique for each of the elastomers before and after the immersion in order to investigate these possible changes. The results are presented and discussed in this section.

Figure 4.4 is an overlay graph displaying the FTIR spectra of the original SBR and SBR after immersion in MEA and MEA/CO_2 solutions. SBR is a copolymer of butadiene and styrene monomers. A butadiene unit can form three different isomers, which are 1,4-cis, 1,4-trans, and 1,2-vinyl and each isomer has its own characteristic FTIR adsorption peaks. The peak at 910 cm^{-1} is attributed to the out of plane (wagging) vibration of CH_2 groups near the double bond group of the vinyl butadiene unit. The out of plane (wagging) vibration of CH groups near the double bond group of 1,4-*trans* unit

occurs at 964 cm^{-1}. For 1,4-cis unit, the characteristic peak is usually present at 699 cm^{-1}; however, it cannot be seen clearly because it is overlapped by the peak of out of plane bending of C-H groups in the aromatic ring of the styrene unit. The sharp but weak peak at 757 cm^{-1} is a result of the deformation of C-H groups in the aromatic ring. The presence of the peak at 1602 cm^{-1} corresponds to the stretching of carbon bonds in the aromatic ring (Gunasekaran, Natarajan, & Kala, 2007; Munteanu & Vasile, 2005; Zhang, He, & Zhou, 2008).

After the immersion of SBR in the loaded and unloaded CO_2 MEA solutions, several new peaks appear. There are some small peaks that appear at 1070 and 1052 cm^{-1} which usually represent the C-O stretching vibration (Ho & Khew, 1999; Ratnam et al., 2000). The small peak at 719 cm^{-1} indicates the N-H wagging vibration, and the sharp peak at 3296 cm^{-1} represents N-H stretching vibration. These two peaks usually appear in secondary amines or amides. The peak at 1641 cm^{-1} results from the amide I band which is the carbonyl stretching vibration. The peaks at 1551, 1515 cm^{-1} represent the amide II band which is mainly due to the N-H bending vibration (Mosadegh-Sedghi et al., 2012; Sedghi et al., 2011). The interference peaks in this area occur due to the intermolecular and intramolecular hydrogen bond N-H (Lin, Chen, & Liang, 1999). The new peaks at 1415 and 1466 cm^{-1} may be from some carboxylate compounds (COO^-), according to Hedzelek et al. (2008).

In conformance with the aforementioned peak assignments, the amide groups appeared in the SBR surface. The amide group might result from the oxidation of SBR followed by reaction with MEA (Mosadegh-Sedghi et al., 2012; Sedghi et al., 2011). This is in agreement with the research of Sedghi et al. (2011) who studied the degradation of

LDPE in 5 M MEA at 25°C for 30 days. They also found an amide group on the LDPE surface.

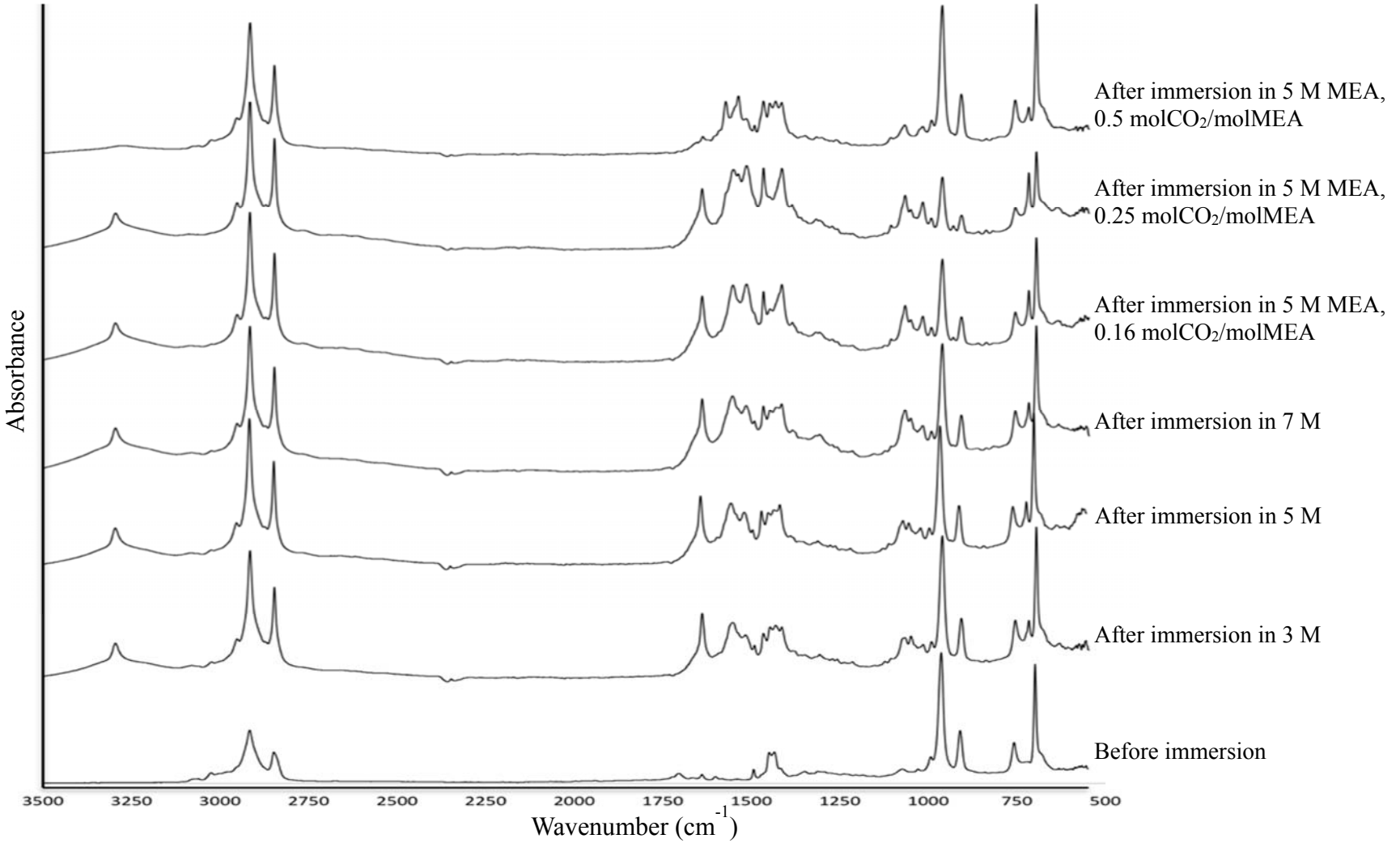

Figure 4.4 FTIR spectra of SBR (Experimental condition: 30 days of immersion, 40°C)

Figure 4.5 shows the effect of MEA concentration (3, 5 and 7 M) on the intensity ratio for determining the relative formation of amide groups. The ratio was calculated from the intensity of the peak at 1641 cm^{-1} which is the vibration mode of amide I band over the intensity of the peak associated with the bending vibration of aromatic ring at 757 cm^{-1}. The peak at 757 cm^{-1} was selected as the internal standard peak because it did not coincide with any other vibration (Jubete et al., 2007). The result shows that with the higher MEA concentration, the formation of amide gradually increased. This is because increasing the MEA concentration can increase the rate of reaction to form amide groups on the SBR surface.

The mass change of SBR increased with the MEA concentration increase. This could result from the chemical adsorption of MEA on SBR during the formation of amide groups. The higher concentration of MEA contributes to increased formation of amide and the increase in mass of SBR during immersion. Figure 4.6 is a plot of the intensity ratio versus CO_2 loading (0.16, 0.25 and 0.5 mol CO_2/mol MEA in 5 M MEA). The dissolution of CO_2 in MEA solutions increases the complexity of the amide formation. At low to medium CO_2 loading, the formation of amide increased with increasing CO_2 concentration in the solutions. This might be as a result that CO_2 is acting as an oxidant. This would result in the increase of the degree of oxidation of SBR with more CO_2 in the solution. The oxidation product then further reacts with free MEA to form amide groups. On the other hand, the intensity ratio decreases at higher CO_2 loading,. CO_2 in solution not only acts as an oxidant to react with SBR but also to oxidize MEA to form a carbamate salt, thus reducing the amount of free MEA as it is consumed by the carbamate

formation reaction. This contributes to the lowering of amide formation at the higher CO_2 loading.

It should be noted that the FTIR result of SBR immersed in MEA/CO_2 solutions (0.16, 0.25 and 0.5 mol CO_2/mol MEA in 5 M MEA) did not agree with the result from the percentage mass change which was shown in the former section. The formation of amide group should bring about an increase in mass of elastomers as new compounds were added on the surface. In contrast, the observed mass of SBR after the immersion in MEA/CO_2 solutions decreased gradually with increasing CO_2 loading. This is because some parts of elastomer were dissolved into the solutions at the same time that mass was added as the reaction for amide formation occurred. The dissolved compounds will be presented and discussed in the section on solution analysis.

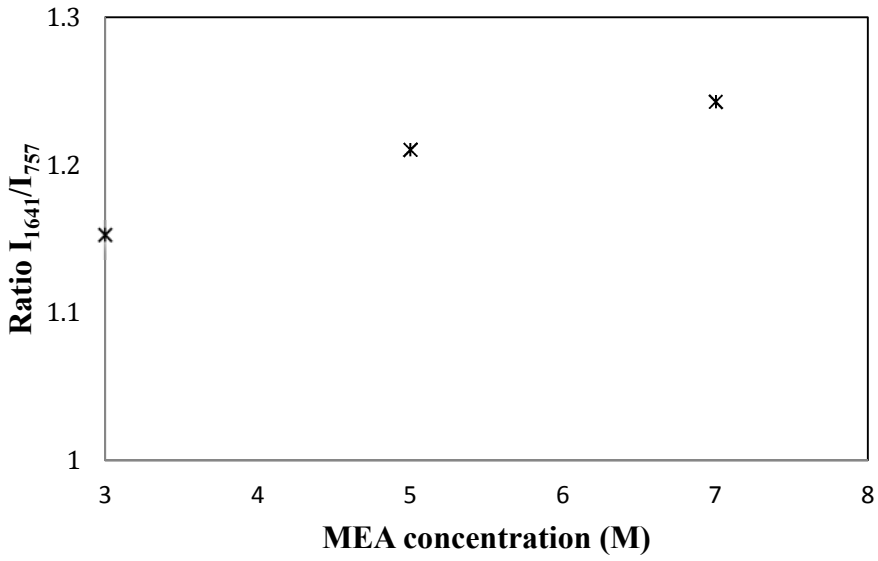

Figure 4.5 Effect of MEA concentration (3, 5, 7 M) on the formation of amide group on SBR surface (Experimental condition: 30 days of immersion, 40°C)

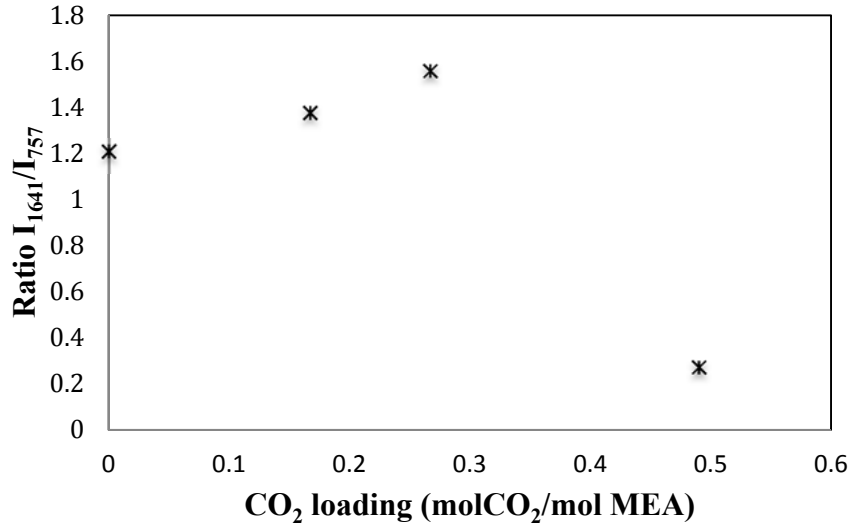

Figure 4.6 Effect of CO_2 loading (0.16, 0.25 and 0.5 mol CO_2/mol MEA in 5 M MEA) on the formation of amide on SBR surface

(Experimental condition: 30 days of immersion, 40°C)

Figure 4.7 shows the FTIR spectra of NR. Before immersion in the solutions, the sharp and strong peak at 843 cm^{-1} for NR corresponds to the out of plane bending vibration of C-H from the *cis* unsaturation configuration while the stretching vibration of C-H from this unit shows up as a small peak at 3080 cm^{-1}. The presence of the sharp and medium peaks at 1375 cm^{-1} and 1446 cm^{-1} is a result of symmetric and asymmetric bending vibration of CH_3. The stretching vibration of C=C shows a peak at 1562 cm^{-1}. The peaks at 2916 cm^{-1} and 2960 cm^{-1} represent symmetric and asymmetric vibrations of C-H from methyl group (Narathichat, Sahakaro, & Nakason, 2010).

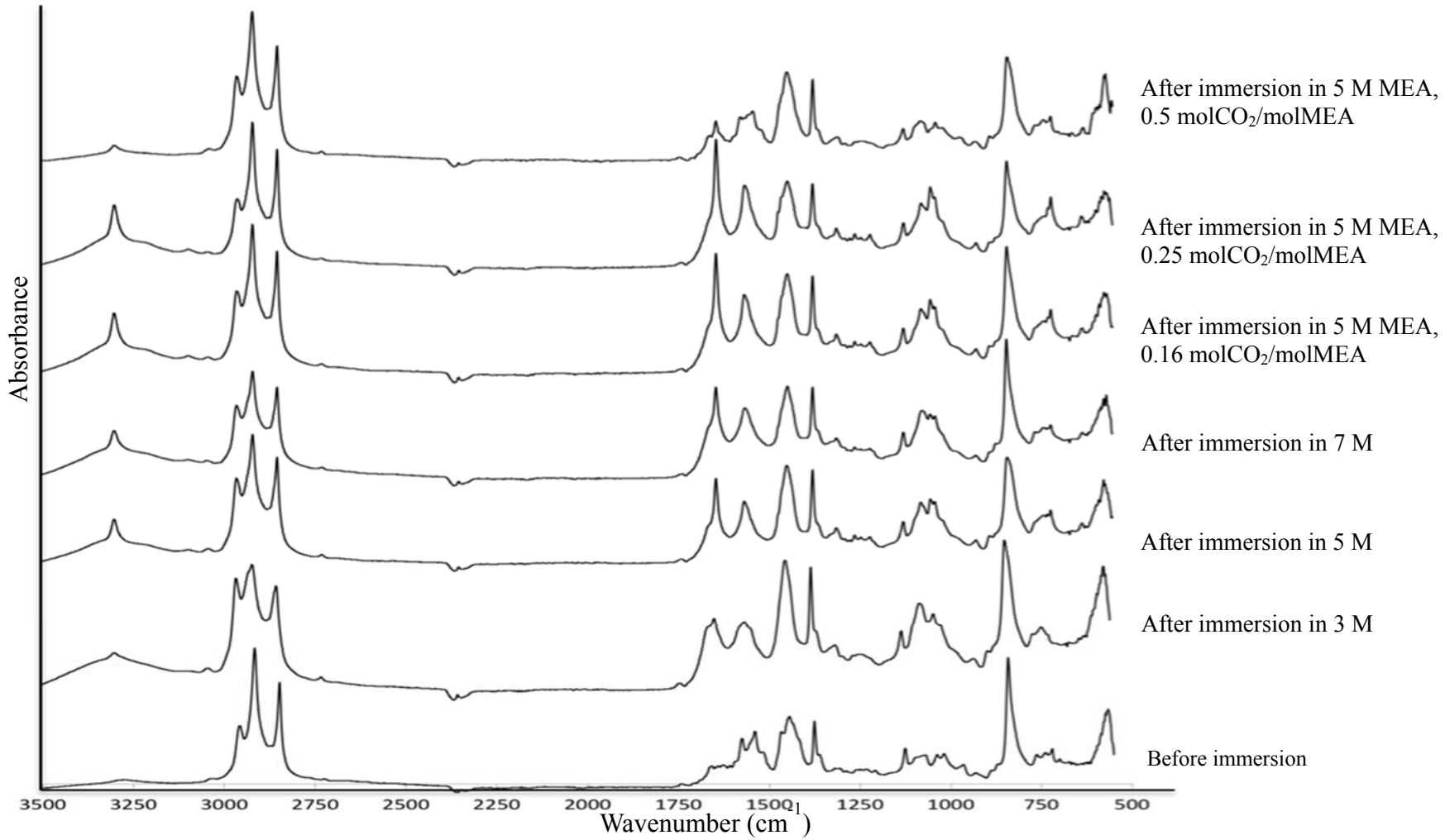

Figure 4.7 FTIR spectra of NR (Experimental condition: 30 days of immersion, 40°C)

After the immersion, new peaks similar to those of SBR that are associated with the amide group also appeared in the FTIR spectra of the NR surface. Moreover, the peaks at 1070 and 1052 cm^{-1} which contribute to C-O stretching vibration found in NR were clearly visible. Figure 4.8 shows the effect of MEA concentration (3, 5 and 7 M) on the intensity ratio which is calculated from the intensity of the peak at 1641 cm^{-1} representing the peak of amide I band. The deformation vibration of methyl group at 1375 cm^{-1} is used as an internal standard peak (Ratnam et al., 2000). It is seen in the figure that the formation of amide groups rapidly increased with increasing MEA concentration. This is because increasing the MEA concentration increased the availability of MEA to react with NR to form amide. The formation of amide can be an important factor in increasing the mass of NR specimens as shown in a previous section. The mass of NR increased after the immersion; however, no definite trend was observed between the percentage mass change and MEA concentration due to the non-uniformity of the porous elastomer samples.

The effect of CO_2 loading (0.16, 0.25 and 0.5 mol CO_2/mol MEA in 5 M) on the amide formation is shown in the Figure 4.9. It shows that the amide group first increases with the concentration of CO_2 due to the ability of CO_2 to act as an oxidant. In the low CO_2 loading, MEA is in excess in the solutions. At high CO_2 loading, the amide group decreased with increasing CO_2 loading. This may be because of the consumption of CO_2 and MEA to form a carbamate salt.

Considering the result from mass change of NR after immersion (0.16, 0.25 and 0.5 mol CO_2/mol MEA in 5 M MEA) from the previous section, the percentage of mass change gradually decreased with increasing CO_2 loading. In an apparent contrast, the

result from FTIR showed the opposite trend. The amide formation increased at low CO_2 loading (0.16 to 0.25 mol CO_2/mol MEA in 5 M MEA) and decreased at high CO_2 loading (0.25 to 0.5 mol CO_2/mol MEA in 5 M MEA). This result can be expected because the formation of amide is not the only cause of the increasing mass; the mass change of NR was affected by physical adsorption. NR has the propensity to absorb and swell in organic solutions. Therefore, the absorption of the solutions in NR played an important role in the increase in mass, as did the chemical reaction.

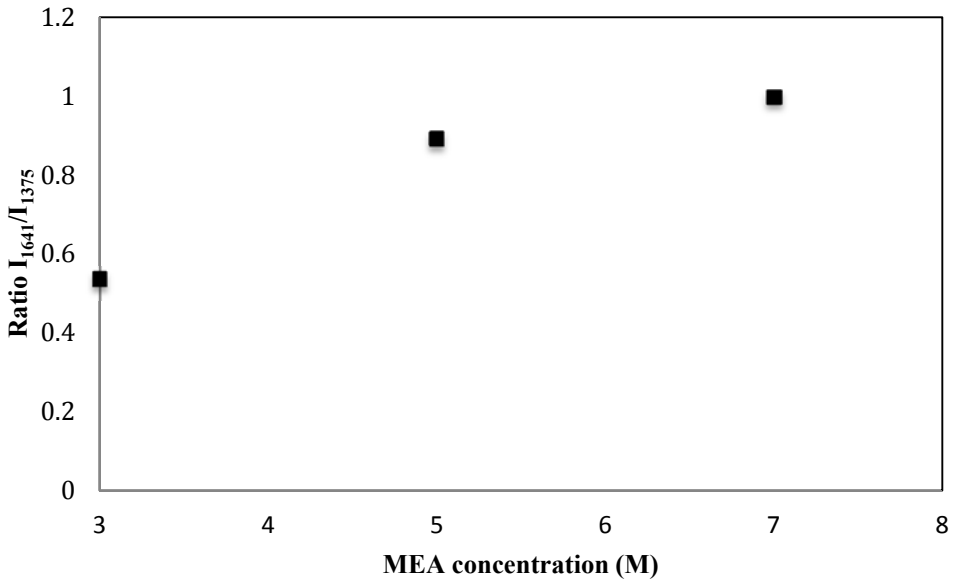

Figure 4.8 Effect of MEA concentration (3, 5, 7 M) on the formation of amide group on NR surface (Experimental conditions: 30 days of immersion, 40 °C)

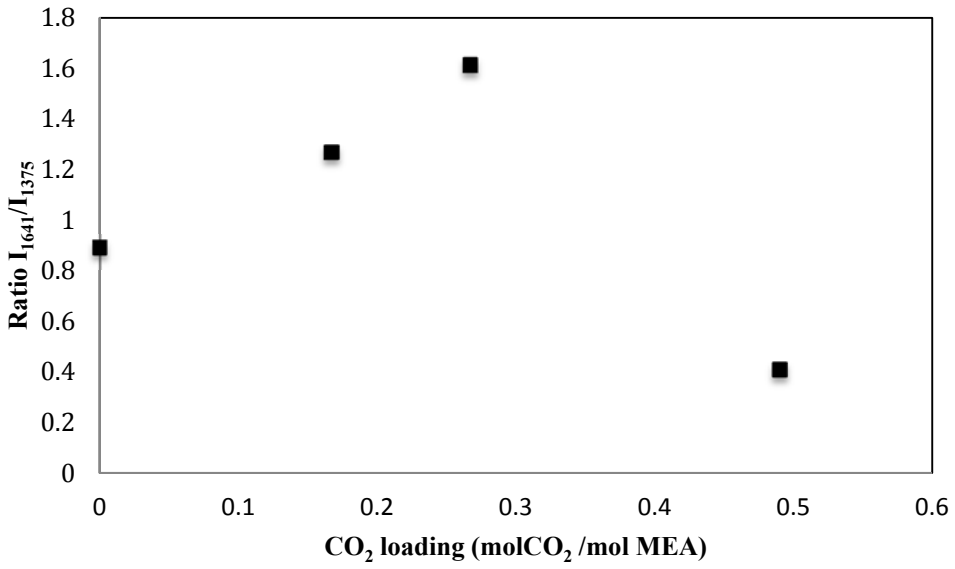

Figure 4.9 Effect of CO_2 loading (0.16, 0.25 and 0.5 mol CO_2/mol MEA in 5 M MEA) on the formation of amide on NR surface

(Experimental conditions: 30 days of immersion, 40°C)

Figure 4.10 is the overlaying of FTIR spectra for EPDM before and after immersion (in 3, 5, 7 M MEA as well as 5 M MEA with 0.16, 0.25 and 0.5 mol CO_2/mol MEA). According to the IR spectra of the original EPDM sample, the presence of $–CH_2$ symmetric and asymmetric stretching bands in methylene units in the saturated hydrocarbon backbone is in the region of 2850 cm^{-1} and 2919 cm^{-1}. The peaks at 1377 cm^{-1} and 1464 cm^{-1} can be attributed to CH symmetric stretching vibration of methyl and CH_2 scissoring vibration of methyl group in propylene units, respectively. The peak at 720 cm^{-1} corresponds to methylene rocking vibration where n>=4 from ethylene units (Tan et al., 2009; Zhao, Li, & Gao, 2008). After the immersion of EPDM in the solutions, some small peaks occurred; however, no major difference was found in the FTIR spectra. This was in agreement with the result of mass change that the mass of EPDM increased after the immersion but the percentages were very small and can be considered to be negligible.

Figure 4.11 presents the FTIR spectra of IIR before and after immersion (in 3, 5 and 7 M MEA as well as 5 M MEA with 0.16, 0.25 and 0.5 mol CO_2/mol MEA). The three strong peaks at 2950, 2916 and 2893 cm^{-1} for the IIR elastomer before immersion represent the stretching vibration from methyl and methylene groups. The peaks at 1470 and 1365 cm^{-1} correspond to asymmetric and symmetric stretching of C-H in CH_3, while the peak at 1388 cm^{-1} is the scissoring bending vibration of C-H in CH_2 from the methylene group. The strong peak at 1229 cm^{-1} is for C-C stretching vibration and the peaks at 922 and 950 cm^{-1} represent the methylene rocking vibration (Dong et al., 2010). From the comparison of the spectra before and after the immersion of SBR in MEA solution, one difference or new peak can be observed. As mentioned in the mass change

results section that showed no significant mass change of IIR in any experimental condition, the backbone of IIR is a saturated carbon chain which exhibits a low chemical reactivity with MEA. Moreover, it has low permeability due to its high content of side chains so that liquid can hardly penetrate into the IIR specimen. This does not only make physical absorption difficult, but also, it lowers the opportunity for chemical reactions to occur.

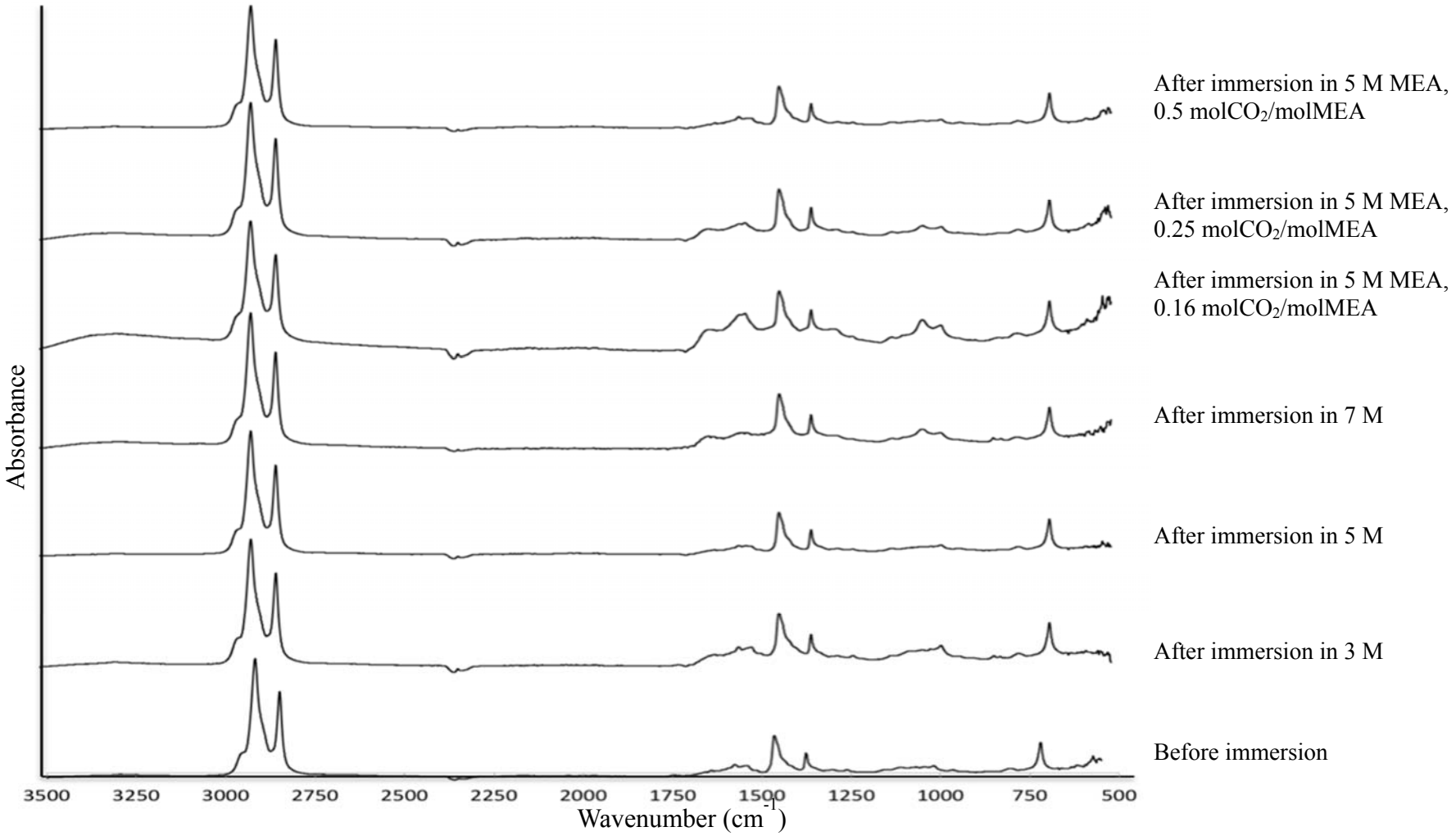

Figure 4.10 FTIR spectra of EPDM (Experimental conditions: 30 days of immersion, 40°C)

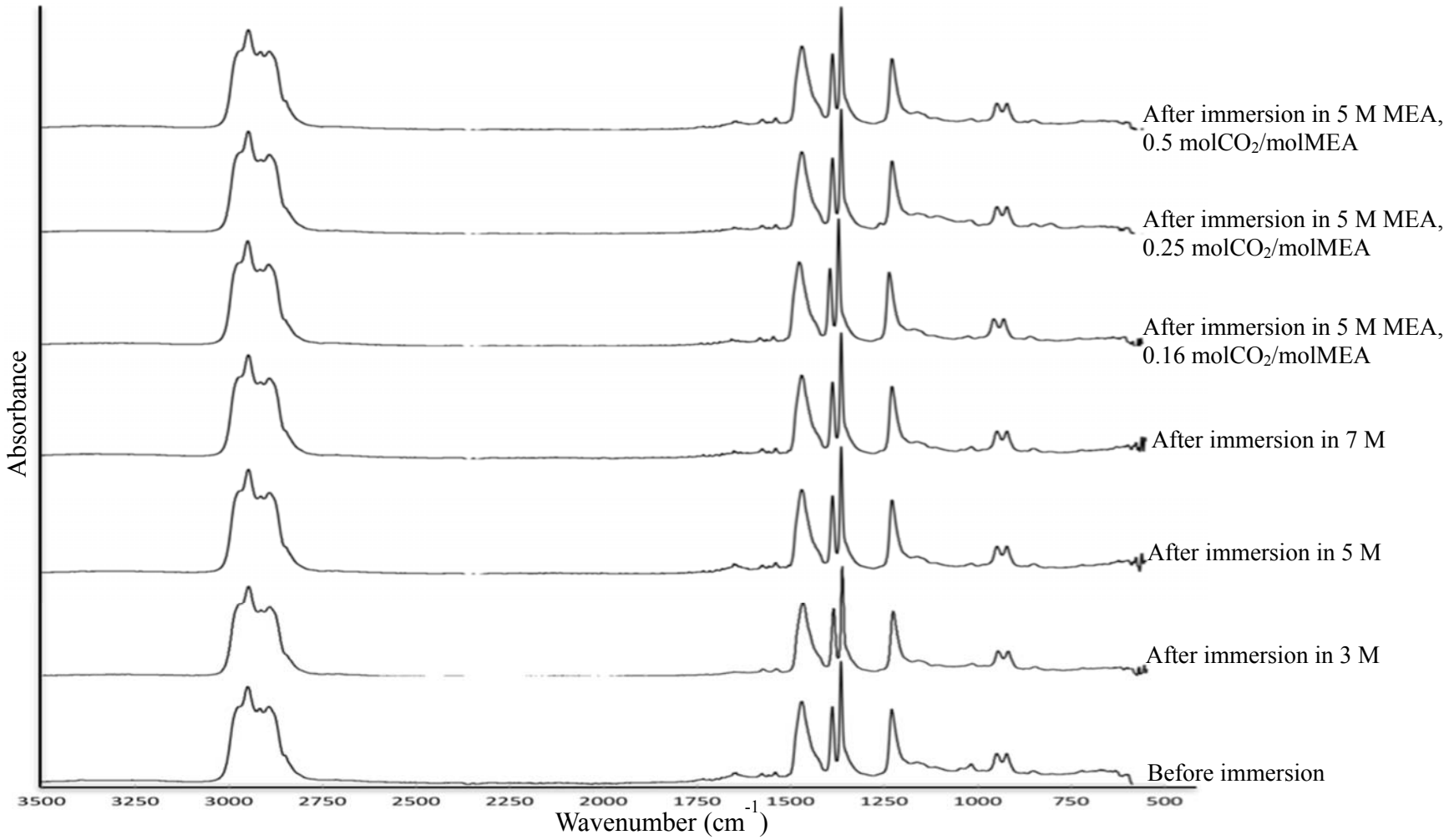

Figure 4.11 FTIR spectra of IIR (Experimental conditions: 30 days of immersion, 40°C)

4.1.4 Solvent Analysis

Elastomer analyses are performed in order to ensure the elastomers have sufficient performance to prevent leakage and keep the process working properly. On the other hand, the analysis of the solutions is also important. The dissolution of some elastomer components in the solutions might cause problems in the CO_2 absorption process such as the production of MEA degradation products or impurities and the occurrence of system plugging.

4.1.4.1 Physical Observation of Solvents

Besides the observation of the elastomers (IIR, EPDM, SBR and NR) before and after immersion as mentioned earlier in section 4.1.1, the changes in the solution due to the immersion were also observed and are discussed in this section. The solutions of MEA (3, 5 and 7 M) after the immersion of IIR, EPDM and NR as well as the solutions of MEA/CO_2 (5 M with 0.16, 0.25 and 0.5 mol CO_2/mol MEA) after the immersion of IIR, EPDM, NR and SBR had minor changes in color. A different result was observed in the solutions of MEA/CO_2 (5 M with CO_2 loading of 0.16, 0.25 and 0.5 mol CO_2/mol MEA) after the immersion of SBR. By observation, it was found that the turbidity of the solutions of MEA/CO_2 increased with increasing CO_2 loading as shown in Figure 4.12 (a). After the solution was allowed to sit, the particles in the solution formed a gel as shown in the Figure 4.12 (b).

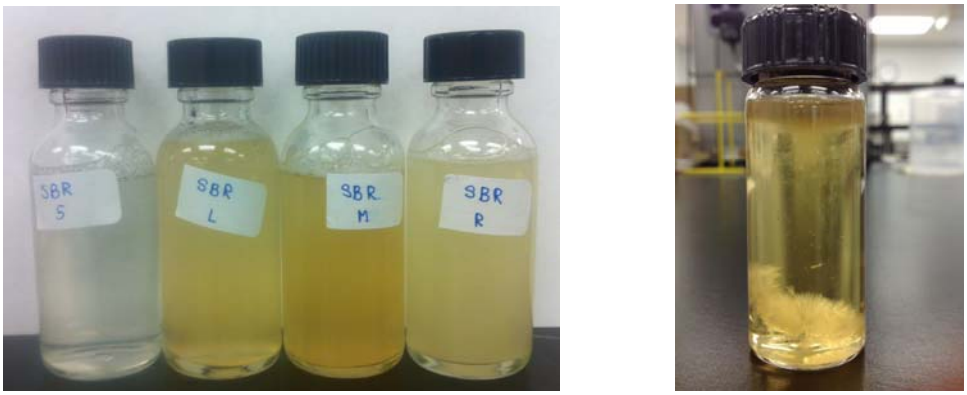

(a) (b)

Figure 4.12 The solutions after the immersion of SBR

(Experimental condition: 30 days of immersion, 40°C)

(a) The solutions after immersion of SBR (5 M MEA and 5 M with 0.16, 0.25 and 0.5 mol CO_2/mol MEA)

(b) The solutions of 5 M MEA with 0.5 mol CO_2/mol MEA after the immersion of SBR

Figure 4.13 shows the NMR ^{1}H spectrum of the sludge obtained from the solution of 5 M MEA with 0.5 mol CO_2/mol MEA after the immersions of SBR for 30 days at 25°C. The chemical shift at 3.678 ppm comes from free MEA (Fan et al., 2009). The small peaks near 7 ppm come from aromatic proton and the chemical shift at 2.4 to 0.8 ppm comes from aliphatic proton (Jukic et al., 2009). From ^{13}C NMR shown in Figure 4.14, the peaks at 61 and 42 ppm indicate the chemical shift of C from CH_2OH and CH_2NH_2 in free MEA (Fan et al., 2009). The chemical shift around 29 to 22 ppm is the carbon long chain from butadiene including *cis*, *trans* and vinyl units (Arantes et al., 2009).

The suspended gel in the solution may be monomers of butadiene and styrene based on the results of ^{1}H NMR and ^{13}C NMR. This can be evidenced by the dissolution of SBR into MEA/CO_2 solutions (5 M MEA and 5 M MEA with 0.16, 0.25 and 0.5 mol CO_2/mol MEA). The solvation of butadiene and styrene monomers caused the reduction in mass of SBR during immersion as shown in the results of mass change from the section 4.1.2, which found that the increase of CO_2 concentration increased the solvation of butadiene and styrene monomers.

To explain the possible interaction during the immersion of SBR in MEA/CO_2 solutions (5 M MEA with 0.16, 0.25 and 0.5 mol CO_2/mol MEA), all the results from mass change, FTIR that indicated the formation of amide compound, as well as the NMR results of the suspended gel need to be considered. The NMR showed that the dissolved CO_2 might have caused oxidation at the double bonds in the SBR chain and cause chain scissoring. The chain scissoring of the SBR results in the dissolution of butadiene and styrene monomers, obviously seen in the form of suspended gel and confirmed by NMR

results. The oxidation reaction not only caused chain scissoring, but also caused the formation of a carbonyl group on the surface of SBR. This carbonyl group reacted further with MEA in the solution to form amide on the surface of the SBR as confirmed by the results from FTIR.

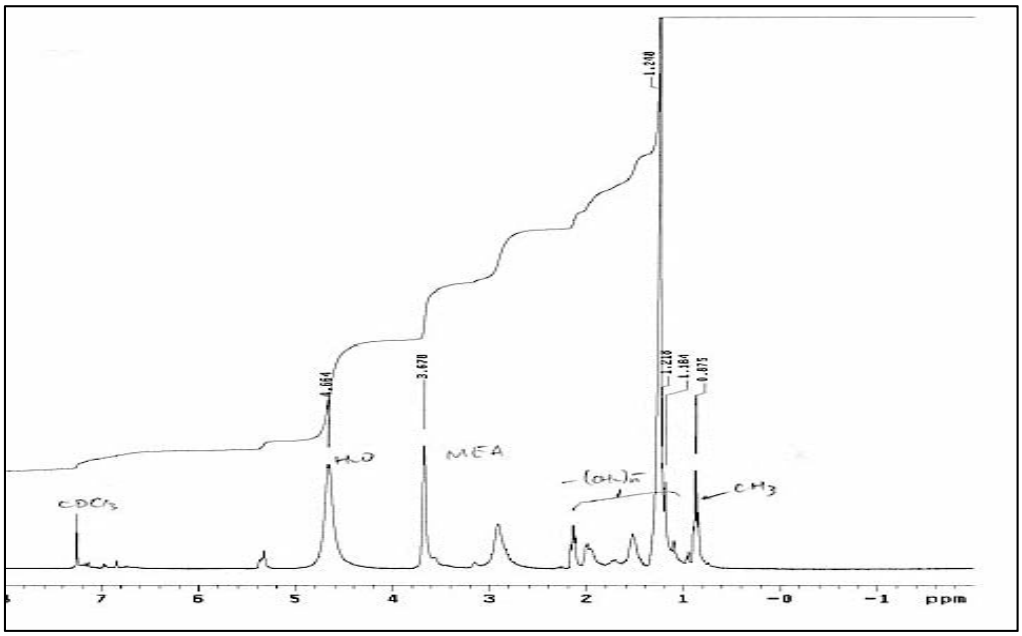

Figure 4.13 ^{1}H MNR spectrum of the sludge from 5 M MEA with 0.5 mol CO_2/mol MEA after immersion of SBR

(Experimental conditions: 30 days of immersion, 40°C)

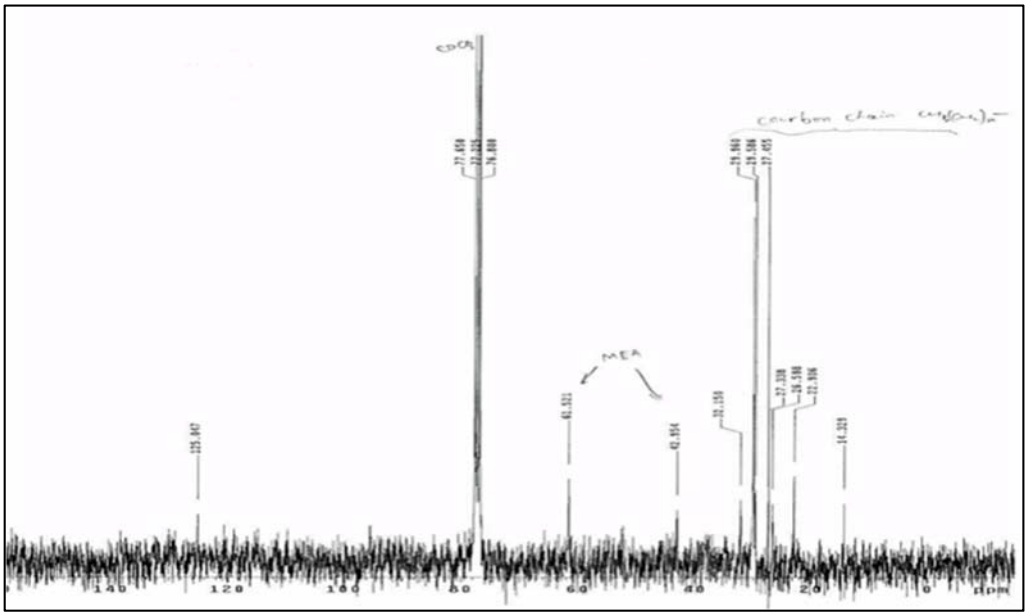

Figure 4.14 ^{13}C MNR spectrum of the sludge from 5 M MEA with 0.5 mol CO_2/mol MEA after immersion of SBR

(Experimental conditions: 30 days of immersion, 40°C)

4.1.4.2 Liquid Analysis by High Performance Liquid Chromatography

The MEA solutions (3, 5 and 7 M) and MEA/CO_2 solutions (5 M MEA with 0.16, 0.25 and 0.5 mol CO_2/mol MEA) after the immersions of elastomers (IIR, EPDM, SBR and NR), and those solutions without elastomer (Reference cells) were analyzed using HPLC in order to investigate new components that might have dissolved from the elastomers.

The investigation of new components with HPLC was obtained using the Diode Array Detector (DAD). From the results, it is not possible to observe any differences between the MEA solutions (3, 5 and 7 M) after the immersion of IIR, EPDM and NR and those solutions from reference cells. Also, the solutions of MEA/CO_2 solutions (5 M MEA with 0.16, 0.25 and 0.5 mol CO_2/mol MEA) after the immersion of EPDM, IIR, NR and SBR did not have significant differences from those of the solutions from reference cells. It is important to note that the chromatograms provided from DAD have the limitation that it only responds to a specific range of compounds such as compounds with double bonds in their structure. The lack of differentiation in the chromatograms of the solutions from the elastomer immersion and the reference solutions might either indicate that there was no component dissolved from the elastomers or that there were some components dissolved from the elastomers but that they cannot be detected by DAD.

One different result was found in the MEA solutions (3, 5 and 7 M) after the immersion of SBR. Two new components, Unknown A and Unknown B, occurred in the solutions as shown in Figure 4.15. The relative quantitative analysis of Unknown A and Unknown B was determined by taking the ratio of peak area of Unknown A or B over the

peak area of imidazole (added into the solutions as an internal standard). The effect of MEA concentration on the relative concentration of Unknown A and Unknown B are shown in Figure 4.16 (a) and Figure 4.16 (b) respectively.

Figure 4.16 (a) is the plot of the ratio of the peak area of A to the peak area of imidazole which represent relative concentration of Unknown A versus the MEA concentrations (3, 5 and 7 M). From the results, the relative concentration of Unknown A increased with MEA concentration. Figure 4.16 (b) shows the effect of MEA concentration (3, 5 and 7 M) on relative concentration of Unknown B. Similar to Unknown A, the relative concentration of Unknown B increased when the MEA concentration increased.

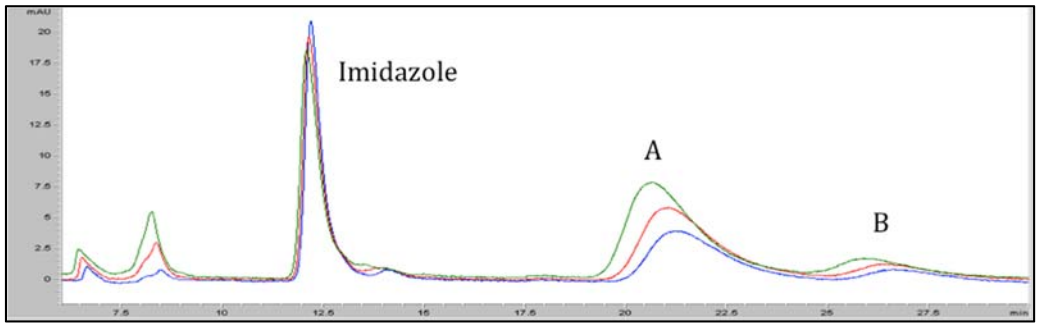

Figure 4.15 HPLC chromatogram of solution after the immersion of SBR in

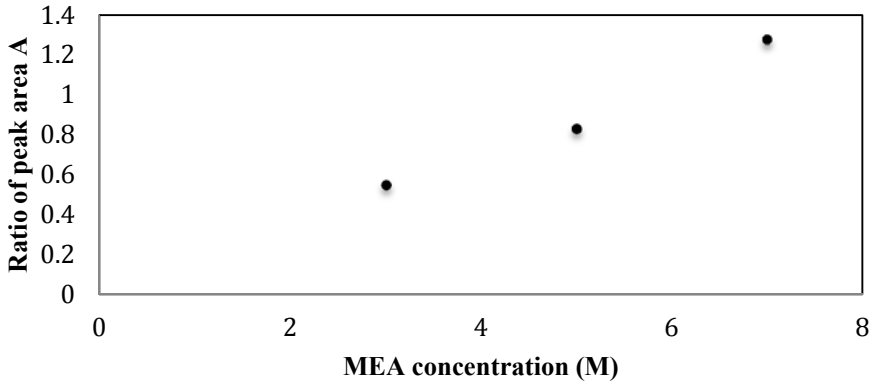

Figure 4.16 (a) Effect of MEA concentration (3, 5 and 7 M) on the concentration of unknown A (Experimental conditions: 30 days of immersion of SBR, 40°C)

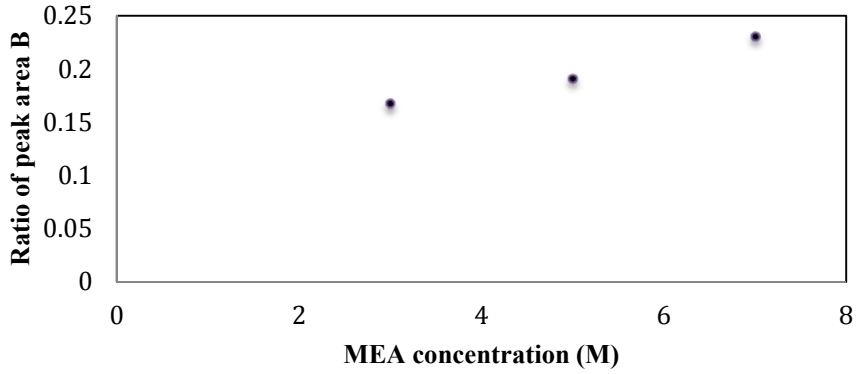

Figure 4.16 (b) Effect of MEA concentration (3, 5 and 7 M) on the concentration of unknown B (Experimental conditions: 30 days of immersion of SBR, 40°C)

The relative concentration of MEA in the solutions (3, 5 and 7 M as well as 5 M with 0.16, 0.25 and 0.5 mol CO_2/mol MEA) after the immersion of the elastomers (IIR, EPDM, SBR and NR) and the reference cells (reference cell 1 for EPDM and SBR, reference cell 2 for NR and IIR) obtained from HPLC with refractive index detector (RID) are shown in Figure 4.17. By comparing the MEA relative concentration from reference cells and those from corresponding cells with elastomers, it was surprising to observe that there were no significant differences MEA concentrations. This would seem to disagree with the results from mass change, FTIR and NMR in the case of SBR and NR. From the former results, SBR and NR had chemical interactions with MEA to form amide groups on their surfaces. As MEA in the solutions was consumed in the reaction to form amide, the MEA concentration should have decreased. In contrast, the MEA concentrations detected from HPLC were constant. This might be because the MEA solutions were in excess compared to the elastomers (Total 6 g. of elastomers in 100 mL of MEA solutions). The amount of MEA that reacted with SBR and NR was very small; thus any change of the MEA concentration would not be observable.

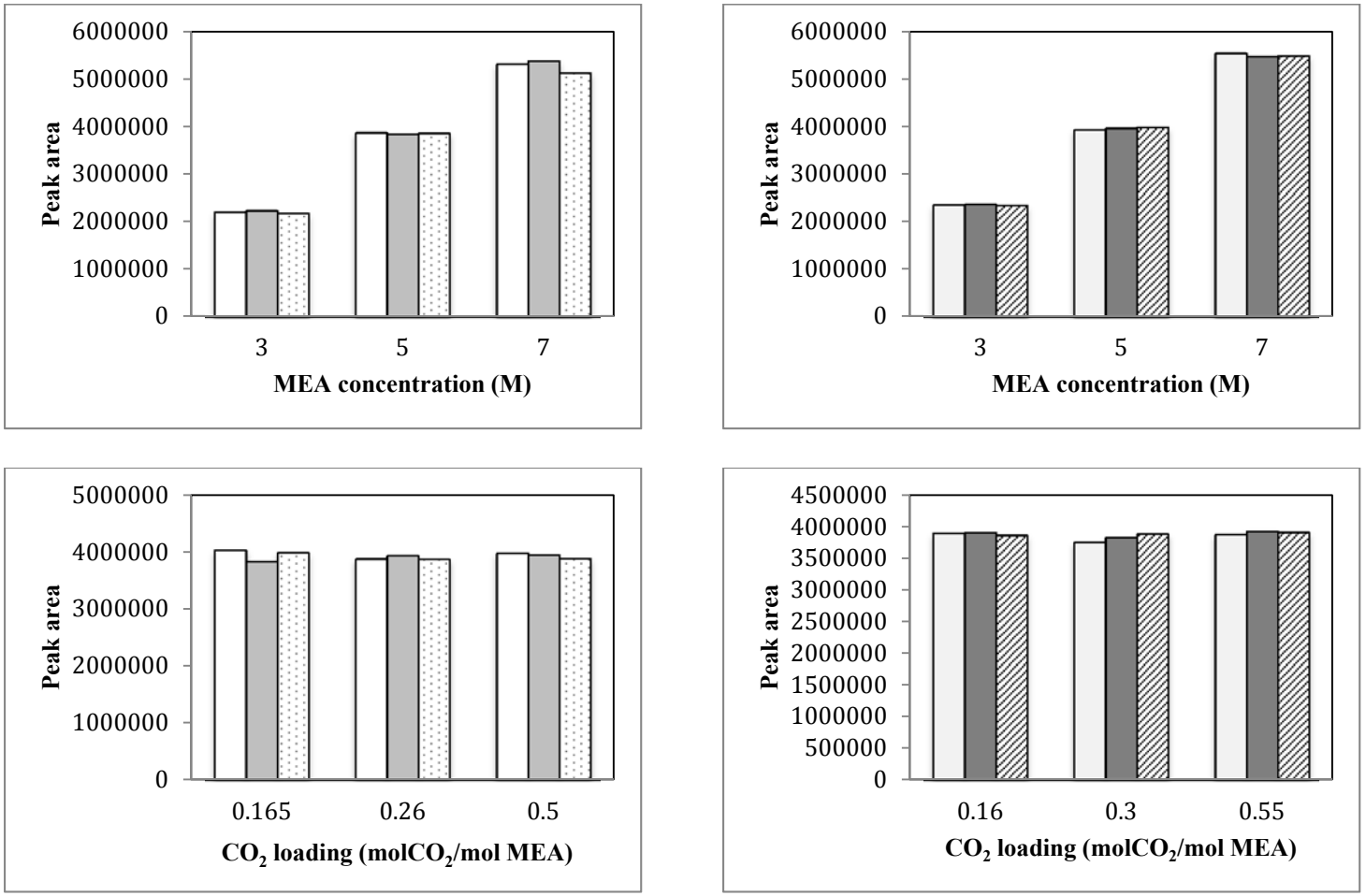

Figure 4.17 Relative concentration of MEA (Experimental condition: 30 days of immersion, 40°C)

4.1.4.3 Miscellaneous Tests

Physical properties including density, viscosity and refractive index of the solutions (3, 5 and 7 M MEA and M MEA with 0.16, 0.25, 0.5 mol CO_2/mol MEA) after the immersion of the elastomers (NR, SBR, EPDM and IIR) and the solutions from the reference cells (Reference cell 1 for EPDM and SBR, Reference cell 2 for NR and IIR) were measured at 25 ^oC. The results are presented in Table 4.1. The comparison between density, viscosity and refractive index of the solutions after the immersion of the elastomers and those of the solutions from the reference cells showed negligible differences.

Table 4.1 Physical properties of the solutions

Cells	MEA Concentration (M)	CO_2 (molCO_2/ mol MEA)	Density $*10^3$(kg/m^3)	Viscosity (cP)	Refractive index
Cell 1*	3	0	1.004	1.512	1.354
	5	0	1.011	2.428	1.370
	7	0	1.017	3.791	1.385
	4.9	0.165	1.045	2.761	1.379
	4.95	0.26	1.066	3.001	1.384
	4.95	0.5	1.115	3.704	1.396
EPDM	3	0	1.004	1.520	1.354
	5	0	1.011	2.425	1.370
	7	0	1.017	3.777	1.385
	4.97	0.166	1.045	2.758	1.379
	4.95	0.264	1.066	2.997	1.384
	4.95	0.5	1.115	3.718	1.396
SBR	3	0	1.004	1.528	1.354
	5	0	1.011	2.432	1.371
	7	0	1.017	3.796	1.385
	4.9	0.167	1.045	2.790	1.379
	4.9	0.267	1.067	3.017	1.385
	4.9	0.49	1.115	3.759	1.396

Cells	MEA Concentration (M)	CO_2 (molCO_2/ mol MEA)	Density *10^3(kg/m^3)	Viscosity (cP)	Refractive index
Cell 2*	3	0	1.005	1.596	1.355
	5	0	1.011	2.460	1.371
	7	0	1.017	3.985	1.387
	4.95	0.163	1.044	2.762	1.379
	4.95	0.295	1.072	3.085	1.386
	4.9	0.543	1.118	3.722	1.396
NR	3	0	1.005	1.608	1.355
	5	0	1.011	2.470	1.371
	7	0	1.017	3.986	1.387
	4.9	0.158	1.044	2.764	1.379
	5.05	0.296	1.072	3.086	1.386
	4.9	0.532	1.119	3.867	1.398
IIR	3	0	1.005	1.590	1.355
	5	0	1.011	2.458	1.371
	7	0	1.017	3.979	1.387
	5	0.164	1.044	2.759	1.379
	5	0.294	1.072	3.093	1.386
	4.95	0.554	1.118	3.728	1.396

*Cell 1 = Reference cell for the solutions after the immersions of EPDM and SBR

*Cell 2 = Reference cell for the solutions after the immersions of NR and IIR

(Experimental conditions: 30 days of immersion, 40°C)

4.2 Commercial Elastomers Testing

After the raw elastomers (IIR, EPDM, SBR and NR) were tested with MEA and MEA/CO_2 solutions at 40 °C, it was determined from all the tests that IIR and EPDM were likely to withstand the solutions, as already presented in previous results. This section reveals the compatibility between commercial IIR, EPDM and PTFE with the solution of MEA with rich CO_2 loading (0.5 mol CO_2/mol MEA in 5 M MEA) at the temperature 40 °C (Absorption temperature) and 120 °C (Stripping temperature).

4.2.1 Mass Change

Figure 4.18 shows the change in mass of IIR, EPDM and PTFE after exposure to the solution of 5 M with 0.5 mol CO_2/mol MEA at 40 and 120 °C for 30 days. The results show that the mass of EPDM and IIR increased after the immersion at both 40 and 120 °C while the mass of PTFE did not significantly change at either temperature.

Basically, commercial elastomers are a complex mixture of base polymer, and fillers and additives such as plasticizer, curing agents, antioxidants, antiozonants and processing aids (Haseeb et al., 2010). The increase in mass can be a result from higher liquid absorption compared to the extraction of soluble components from the elastomers. The absorption of liquid into the elastomers can be either chemical or physical absorption. In the case of EPDM and IIR, the chemical resistance of base polymers (Raw elastomer of EPDM and IIR) to MEA and MEA/CO_2 solutions at 40 °C were tested in the previous section. It showed that raw elastomers of EPDM and IIR did not react with the MEA and MEA/CO_2 solutions. Therefore, the increase of mass of commercial EPDM and IIR at 40 °C might be a result of physical absorption or chemical reaction between

the solution with fillers and additives compared to the extraction of soluble components that might also occur.

PTFE, which is considered as a thermosetting plastic has a crystalline structure. MEA solution can hardly diffuse into the packed structure of PTFE. Moreover, it has the outstanding ability of high chemical resistance due to the bonds between carbon atoms and fluorine atoms; thus, the chemical reaction between PTFE and the MEA solution is difficult to occur. These might be the reasons why the mass of PTFE remained constant after the immersion. Even when the temperature was increased, the mass of PTFE remained almost constant. On the other hand, with increasing temperature, changes in mass increased for EPDM and IIR. For an increase in temperature from 40 to 120 °C, the percentage mass change increased from 2.1% to 44.3% for EPDM and 2.3% to 43.1% for IIR. This can be because the increase of temperature facilitated the diffusion rate of the solution in commercial EPDM and IIR (Haseeb et al., 2010).

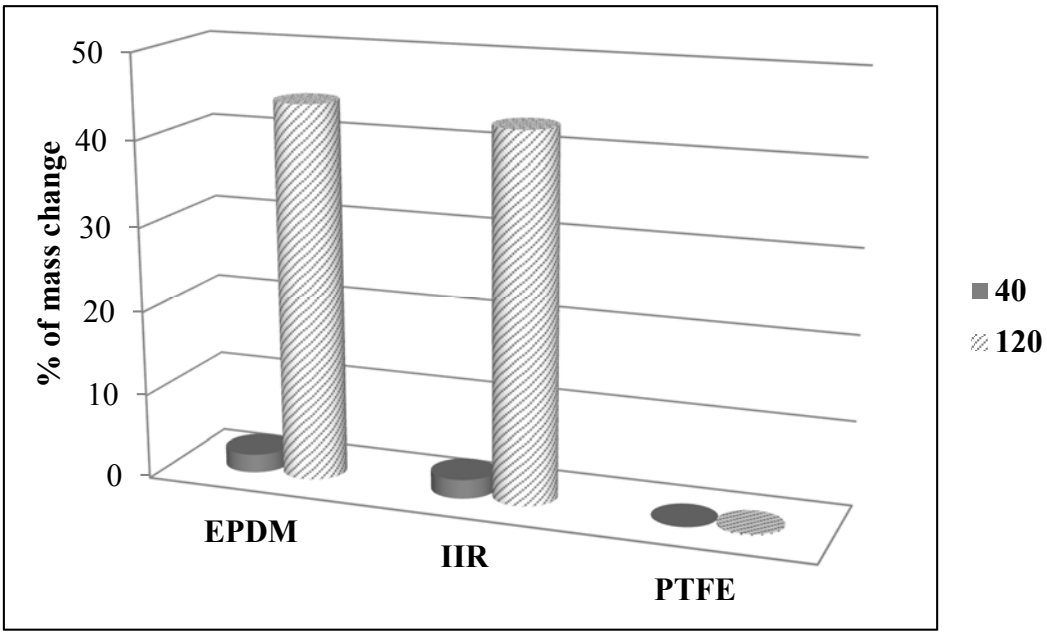

Figure 4.18 Mass change of commercial EPDM, IIR, and PTFE after immersion in 5 M with 0.5 mol CO_2/mol MEA at 40 and 120 °C for 30 days

4.2.2 Mechanical Properties

This section reveals the effects of the immersions (in 5 M with 0.5 mol CO_2/mol MEA) and the immersion temperatures (40 and 120 °C) on mechanical properties of commercial EPDM, IIR and PTFE. Figures 4.19 and 4.20 show comparisons of hardness and tensile strengths of commercial EPDM, IIR and PTFE obtained before immersion and after immersion. At 40 °C, the hardness of commercial EPDM, IIR and PTFE had no significant change. With the increase in immersion temperature to 120 °C, the hardness of PTFE still remained almost constant, while the hardness of EPDM and IIR rapidly decreased.

After exposed to the solution at 40 °C, Figure 4.20 shows that the tensile strength of commercial EPDM decreased slightly. There is a drastic decrease in tensile strength with an increase in temperature. There was no significant difference in tensile strength for commercial IIR between before and after it was exposed to the solution at 40°C; however, the tensile strength of IIR rapidly dropped after exposed to the solution at 120 °C. Unlike those of EPDM and IIR, the tensile strength of PTFE did not have any significant change after the immersion. The changes of tensile strength and hardness of commercial EPDM and IIR are in agreement with the results of mass changes. The absorption of solution reduced the mechanical properties of the material (Alves, Mello, & Medeiros, 2013).

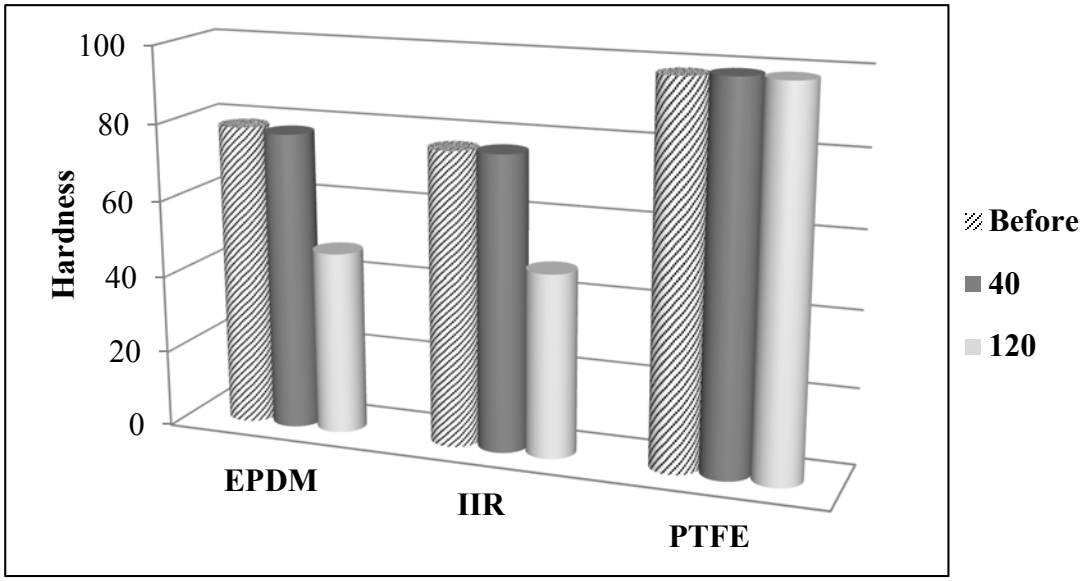

Figure 4. 19 Hardness of commercial EPDM, IIR, and PTFE

(5 M with 0.5 mol CO_2/mol MEA at 40 and 120 °C for 30 days)

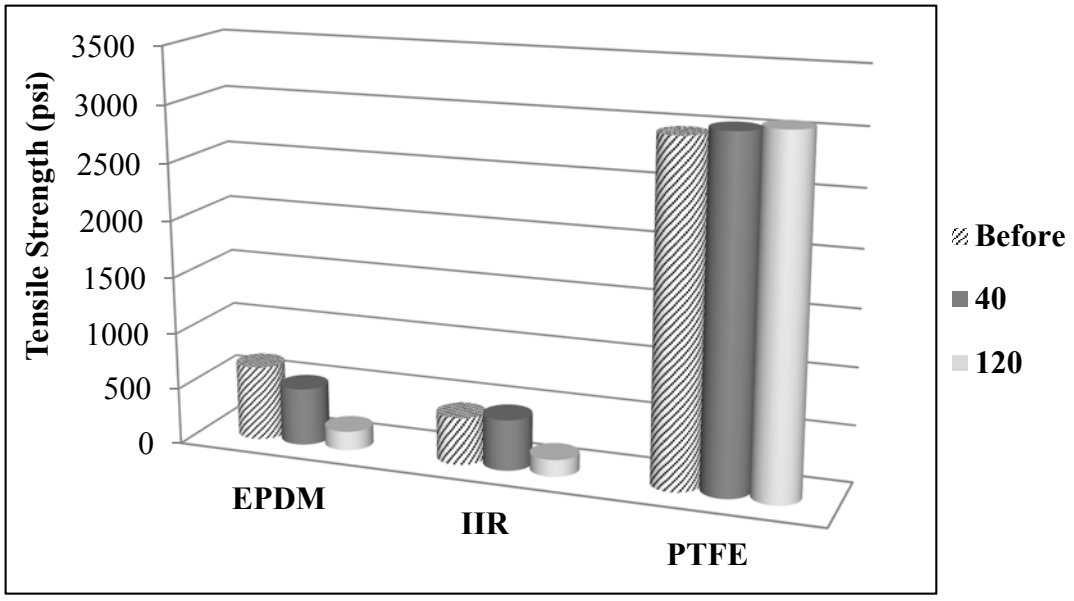

Figure 4. 20 Hardness of commercial EPDM, IIR, and PTFE

(5 M with 0.5 mol CO_2/mol MEA at 40 and 120 °C for 30 days)

4.2.3 Surface Degradation of Commercial Elastomers

The SEM images of the surfaces of commercial EPDM and IIR before immersion and after immersion in 5 M MEA with 0.5 mol CO_2/mol MEA at 120 °C for 30 days were captured by SME are shown in the Figure 4.21 and 4.22. After the immersion of commercial EPDM, the surface turned rougher. The similar results were also found for commercial IIR. The rougher surface was an evidence of deterioration of commercial EPDM and IIR due to exposure to the solution at 120 °C. This result agreed with the results of hardness and tensile strength that significantly dropped after the immersion at high temperature.

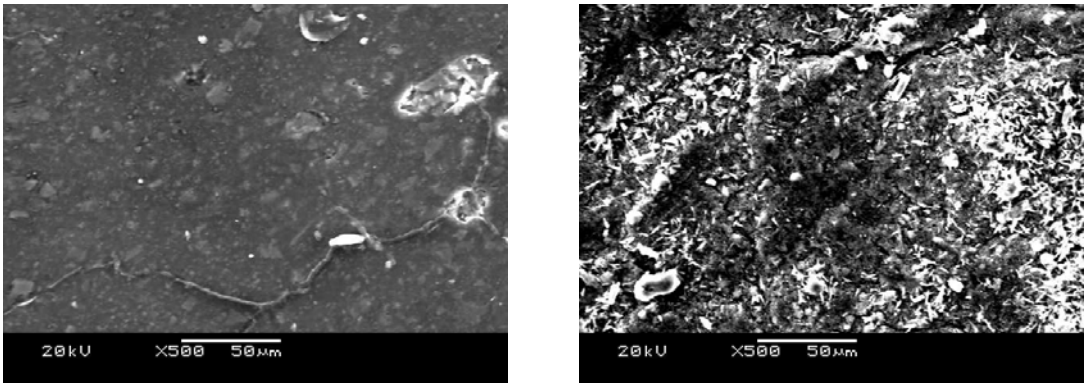

(a) (b)

Figure 4.21 SEM images of commercial EPDM (a) Before immersion, (b) After immersion in 5 M MEA with 0.5 mol CO_2/mol MEA at 120 °C for 30 days

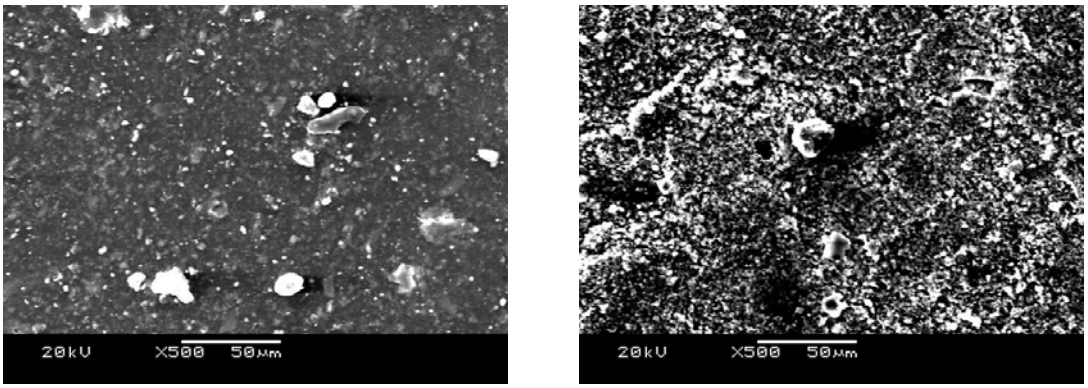

(a) (b)

Figure 4.22 SEM images of commercial IIR (a) Before immersion, (b) After immersion in 5 M MEA with 0.5 mol CO_2/mol MEA at 120 °C for 30 days

CHAPTER V

CONCLUSIONS AND RECOMMENDATIONS

5.1 Conclusions

This thesis aims to search for a high performance material that can be used for sealing applications in an amine-based CO_2 capture process. In this study, the screening of elastomers that are likely to withstand MEA solutions was performed by first collecting compatibility tables from elastomer suppliers. Then, the chemical resistance of the selected raw elastomers was investigated. Finally, to ensure that the chosen raw elastomers were capable of being used in a CO_2 absorption and stripping process, commercial elastomers originating from the selected raw material was tested at both the absorber and regenerator temperatures. The conclusions from this study can be summarized as follows.

1. Based solely on compatibilities tables provided from elastomer suppliers, the most recommended elastomers that can be used for amine-based CO_2 capture process are EPDM, IIR, SBR and NR.

2. The study of chemical resistance of raw elastomers to the solutions of MEA (3, 5 7 M) and MEA/CO_2 (0.16, 0.25, 0.5 mol CO_2/mol MEA in MEA 5 M) at 40 °C show that EPDM and IIR have better chemical resistance as compared to SBR and NR. The experiment results are summarized as follow:

- After the immersion of EPDM and IIR into MEA and MEA/CO_2 solutions, mass of EPDM slightly increased due to physical absorption while the mass of IIR remained constant. Moreover, from FTIR interpretation, there was no

significant change in chemical structure of EPDM and IIR. Therefore, raw EPDM and IIR can be recommended to be the base polymers used in sealing material in an amine-based CO_2 capture process.

- Raw SBR and NR have poor chemical resistance to MEA and MEA/CO_2 solutions because they can react with the MEA solutions to form amides on their surfaces that can be seen from FTIR spectra. The amides might occur from the oxidation of the elastomers. The products from oxidation reaction then react further with MEA forming amides as the final product on the elastomer surfaces.
- A higher MEA concentration contributed to an increase in the formation of amides resulting in an increase in mass of SBR and NR after the immersion. This is because the higher MEA concentrations, the more the MEA molecules made available for the amide formation reaction.
- With the addition of CO_2 into MEA solution, there was the dissolution of styrene and butadiene monomers observed for SBR which resulted in a decrease in SBR mass after the immersions. The solvation of monomer was not observed for NR.
- At low CO_2 concentration, the formation of amides on SBR and NR surfaces increased because CO_2 accelerates oxidation reaction. At high CO_2 concentration, the formation of amide started to decrease because MEA in the solution was consumed in the competing carbamate formation reaction.

3. From the study of the compatibility of commercial EPRM, IIR and PTFE with the MEA solution used in CO_2 capture process, PTFE showed excellent compatibility. It

would be the most recommended material for used in both the absorber and regenerator. For EPDM and IIR, these might be used in the absorber as only small changes on their masses and physical properties were observed at the absorber temperature. At the regenerator temperature, EPDM and IIR are not recommended in the regenerator because their masses increased, their physical properties decreased and surface deteriorated after contact with the solution.

5.2 Recommendations for Future Work

- Even though MEA is the most popular solvents for CO_2 absorption, mixed amine solvents based on MEA, such as MEA/MDEA or MEA/PZ have become popular today. Therefore, future work should focus on different amine solutions or their mixtures.
- O_2 is one of the most dangerous compounds to polymer material as it can cause oxidation reaction. Thus, the effect of O_2 in amine solutions on the degradation of seal material should be studied in future work.
- The knowledge obtained from this work is not only useful in power generation plants, but also, it can be applied to similar process such as natural gas separation. However, the effect of hydrogen sulfide on the degradation of seal material should be studied in this case.

REFERENCES

Aboudheir, A., Tontiwachwuthikul, P., Chakma, A., & Idem, R. (2003). Kinetics of the reactive absorption of carbon dioxide in high CO_2-loaded, concentrated aqueous monoethanolamine solutions. *Chem. Eng. Sci., 58*(23), 5195-5210.

Allen, N. S. (1992). *Fundamentals of Polymer Degradation and Stabilization*: Springer.

Allen, N. S., Barcelona, A., Edge, M., Wilkinson, A., Merchan, C. G., & Ruiz Santa Quiteria, V. (2004). Thermal and photooxidation of high styrene-butadiene copolymer (SBC). *Polym. Degrad. Stab., 86*(1), 11-23.

Alves, S. M., Mello, V. S., & Medeiros, J. S. (2013). Palm and soybean biodiesel compatibility with fuel system elastomers. *Tribol Int, 65*(0), 74-80.

Andersen, H. (2005). Pre-Combustion Decarbonisation Technology Summary. *Carbon Dioxide Capture for Storage in Deep Geologic Formations* (pp. 203-211). Amsterdam: Elsevier Science.

Arantes, T. M., Leao, K. V., Tavares, M. I. s. B., Ferreira, A. G., Longo, E., & Camargo, E. R. (2009). NMR study of styrene-butadiene rubber (SBR) and TiO_2 nanocomposites. *Polym. Test., 28*(5), 490-494.

Aroonwilas, A., Veawab, A., & Tontiwachwuthikul, P. (1999). Behavior of the Mass-Transfer Coefficient of Structured Packings in CO2 Absorbers with Chemical Reactions. *Ind. Eng. Chem. Res., 38*(5), 2044-2050.

Baah, C. A., & Baah, J. I. (2001). Effect of organic reagents on neoprene, nitrile and natural rubbers. *Mater. Des., 22*(5), 403-405.

Baah, C. A., Baah, J. I., Gianadda, P., & Fisher, C. (2000). Behavior of polysulphide rubber (thiokol A) in organic acid solutions. *Mater. Des., 21*(3), 211-215.

Chaikumpollert, O., Sae-Heng, K., Wakisaka, O., Mase, A., Yamamoto, Y., & Kawahara, S. (2011). Low temperature degradation and characterization of natural rubber. *Polym. Degrad. Stab., 96*(11), 1989-1995.

Chakma, A. (1995). An energy efficient mixed solvent for the separation of CO_2. *Energy Convers. Manage., 36*(6), 427-430.

Chandrasekaran, C. (2009). *Rubber Seals for Fluid and Hydraulic Systems*: Elsevier Science.

Chandrasekaran, V. C. (2009). *Tank Linings for Chemical Process Industries*: iSmithers Rapra Publishing.

Horwitz, W. (1975). Association of Official Analytical Chemists. (AOAC) meth-ods, 12th ed. (12th edition ed.), George Banta.

Ciesielsky, A. (1999). *An introduction to rubber technology*. iSmithers Rapra Publishing.

Conley, R. T. (1972). *Infrared spectroscopy*: Allyn and Bacon.

Do, T.-T., Celina, M., & Fredericks, P. M. (2002). Attenuated total reflectance infrared microspectroscopy of aged carbon-filled rubbers. *Polym. Degrad. Stab., 77*(3), 417-422.

Dong, X. C., Zhang, Q. L., Feng, Y., Xing, Z., & Zhao, J. R. (2010). Preparation and Properties of Isobutylene-isoprene Rubber Containing Multifunctional Groups. *Iran Polym J., 19*(10), 771-779.

European Sealing Association (ESA). (1998). Guidelines for safe seal usage-Flanges and Gaskets. *Report No. ESA/FSA, 9*(98), 1-40.

Fan, G.-j., Wee, A. G. H., Idem, R., & Tontiwachwuthikul, P. (2009). NMR Studies of Amine Species in MEA-CO_2-H_2O System: Modification of the Model of Vapor-Liquid Equilibrium (VLE). *Ind. Eng. Chem. Res., 48*(5), 2717-2720.

Georgoulis, L. B., Morgan, M. S., Andrianopoulos, N., & Seferis, J. C. (2005). Swelling of polymeric glove materials during permeation by solvent mixtures. *J. Appl. Polym. Sci., 97*(3), 775-783.

Gunasekaran, S., Natarajan, R., & Kala, A. (2007). FTIR spectra and mechanical strength analysis of some selected rubber derivatives. *Spectrochim. Acta, Part A, 68*(2), 323-330.

Haseeb, A. S. M. A., Jun, T. S., Fazal, M. A., & Masjuki, H. H. (2011). Degradation of physical properties of different elastomers upon exposure to palm biodiesel. *Energy, 36*(3), 1814-1819.

Haseeb, A. S. M. A., Masjuki, H. H., Siang, C. T., & Fazal, M. A. (2010). Compatibility of elastomers in palm biodiesel. *Renewable Energy, 35*(10), 2356-2361.

Hedzelek, W., Wachowiak, R., Marcinkowska, A., & Domka, L. (2008). Infrared spectroscopic identification of chosen dental materials and natural teeth. *Acta Phys. Pol. A, 114*(2), 471.

Herzog, H. (2009). *A Research Program for Promising Retrofit Technologies.* Paper presented at the MIT Symposium on Retrofitting of Coal-fired Power Plants for Carbon Capture.

Ho, C., & Khew, M. (1999). Surface characterisation of chlorinated unvulcanised natural rubber latex films. *Int. J. Adhes Adhes., 19*(5), 387-398.

Hoff, K. a. (2003). *Modeling and experimental study of carbon dioxide absorption in a membrane contactor*. Norwegian University of Science and Technology, Norway.

Statistics, I. E. A. (2011). CO2 emissions from fuel combustion-highlights.*IEA, Paris http://www.iea.org/co2highlights/co2highlights.pdf. Cited July*.

Ito, M. (2007). Degradation of elastomer by heat and/or radiation. *Nucl. Instrum. Methods Phys. Res., Sect B, 265*(1), 227-231.

Jubete, E., Liauw, C. M., Jacobson, K., & Allen, N. S. (2007). Degradation of carboxylated styrene butadiene rubber based water born paints. Part 1: Effect of talc filler and titania pigment on UV stability. *Polym. Degrad. Stab., 92*(8), 1611-1621.

Jukić, A., Rogošić, M., Franjić, I., & Šoljić, I. (2009). Molecular interaction in some polymeric additive solutions containing styrene-hydrogenated butadiene copolymer. *Eur. Polym. J., 45*(9), 2594-2599.

Kittel, J., Idem, R., Gelowitz, D., Tontiwachwuthikul, P., Parrain, G., & Bonneau, A. (2009). Corrosion in MEA units for CO_2 capture: Pilot plant studies. *Energy Procedia, 1*(1), 791-797.

Kohl, A. L., & Nielsen, R. (1997). *Gas Purification*: Elsevier Science.

Lehrle, R. S., & Pattenden, C. S. (1998). Gamma irradiation of a polyisobutylene rubber: effects on the molecular weight and the subsequent thermal stability. *Polym. Degrad. Stab., 62*(2), 211-223.

Leja, K., & Lewandowicz, G. y. Polymer biodegradation and biodegradable polymers‚Äì a review.

Lin, S.-Y., Chen, K.-S., & Liang, R.-C. (1999). Thermal micro ATR/FT-IR spectroscopic system for quantitative study of the molecular structure of poly(N-isopropylacrylamide) in water. *Polymer, 40*(10), 2619-2624.

Linhares, F. N., Corr√™a, H. L. o., Khalil, C. N., Amorim Moreira Leite, M. r. C., & Guimar√£es Furtado, C. R. (2013). Study of the compatibility of nitrile rubber with Brazilian biodiesel. *Energy, 49*(0), 102-106.

Mandal, B. P., Guha, M., Biswas, A. K., & Bandyopadhyay, S. S. (2001). Removal of carbon dioxide by absorption in mixed amines: modelling of absorption in aqueous MDEA/MEA and AMP/MEA solutions. *Chem. Eng. Sci., 56*(21), 6217-6224.

Mitra, S., Ghanbari-Siahkali, A., Kingshott, P., Rehmeier, H. K., Abildgaard, H., & Almdal, K. (2006). Chemical degradation of crosslinked ethylene-propylene-diene rubber in an acidic environment. Part I. Effect on accelerated sulphur crosslinks. *Polym. Degrad. Stab., 91*(1), 69-80.

Mosadegh-Sedghi, S., Brisson, J. e., Rodrigue, D., & Iliuta, M. C. (2012). Morphological, chemical and thermal stability of microporous LDPE hollow fiber membranes in contact with single and mixed amine based CO_2 absorbents. *Sep. Purif. Technol., 96*(0), 117-123.

Munteanu, S., & Vasile, C. (2005). Spectral and thermal characterization of styrene-butadiene copolymers with different architectures. *J. Optoelectron. Adv. Materials, 7*(6), 3135.

Nakamura, T., Chaikumpollert, O., Yamamoto, Y., Ohtake, Y., & Kawahara, S. (2011). Degradation of EPDM seal used for water supplying system. *Polym. Degrad. Stab., 96*(7), 1236-1241.

Narathichat, M., Sahakaro, K., & Nakason, C. (2010). Assessment degradation of natural rubber by moving die processability test and FTIR spectroscopy. *J. Appl. Polym. Sci., 115*(3), 1702-1709.

Øi, L. E. (2007, October). Aspen HYSYS simulation of CO_2 removal by amine absorption from a gas based power plant. In *The 48th Scandinavian Conference on Simulation and Modeling (SIMS 2007), 30-31 October, 2007, Göteborg (Särö)* (pp. 73-81).

Parker, D. B. V. (1974). *Polymer Chemistry*: Applied Science Publ.

Pekcan, O., & Ugur, S. (2002). Molecular weight effect on polymer dissolution: a steady state fluorescence study. *Polymer, 43*(6), 1937-1941.

Philip A. Schweitzer, P. E. (2010). *Corrosion of Polymers and Elastomers*: Taylor & Francis.

Raju, G., Reddy, B. M., & Park, S.-E. (2012). Utilization of carbon dioxide in oxidative dehydrogenation reactions. *Indian J. Chem. Sect A., 51*(9), 1315.

Ratnam, C. T., Nasir, M., Baharin, A., & Zaman, K. (2000). Electron beam irradiation of epoxidized natural rubber: FTIR studies. *Polym. Int., 49*(12), 1693-1701.

Rubin, E. S., Regina, U. o., Canada, C. N. R., R, I. G. G., & Programme, D. (2005). *Greenhouse gas control technologies: proceedings of the 7th International Conference on Greenhouse Gas Control Technologies : 5-9 September 2004, Vancouver, Canada*: Elsevier.

Scheffknecht, G. n., Al-Makhadmeh, L., Schnell, U., & Maier, J. r. (2011). Oxy-fuel coal combustion,ÄîA review of the current state-of-the-art. *Int. J. Greenhouse Gas Control, 5, Supplement 1*(0), S16-S35.

Sedghi, S. M., Brisson, J. e., Rodrigue, D., & Iliuta, M. C. (2011). Chemical alteration of LDPE hollow fibers exposed to monoethanolamine solutions used as absorbent for CO_2 capture process. *Sep. Purif. Technol., 80*(2), 338-344.

Supap, T., Idem, R., Tontiwachwuthikul, P., and Saiwan, C. (2006). Analysis of monoethanolamine and its oxidative degradation products during CO_2 absorption from flue gases: A comparative study of GC-MS, HPLC-RID, and CE-DAD analytical techniques and possible optimum combinations. *Ind. Eng. Chem. Res., 45*(8), 2437-2451.

Tan, J., Chao, Y. J., Wang, H., Gong, J., & Van Zee, J. W. (2009). Chemical and mechanical stability of EPDM in a PEM fuel cell environment. *Polym. Degrad. Stab., 94*(11), 2072-2078.

Trakarnpruk, W., & Porntangjitlikit, S. (2008). Palm oil biodiesel synthesized with potassium loaded calcined hydrotalcite and effect of biodiesel blend on elastomer properties. *Renewable Energy, 33*(7), 1558-1563.

Wang, M., Lawal, A., Stephenson, P., Sidders, J., & Ramshaw, C. (2011). Post-combustion CO_2 capture with chemical absorption: A state-of-the-art review. *Chem. Eng. Res. Des., 89*(9), 1609-1624.

Wang, R., Li, D. F., Zhou, C., Liu, M., & Liang, D. T. (2004). Impact of DEA solutions with and without CO_2 loading on porous polypropylene membranes intended for use as contactors. *J. Membr. Sci., 229*(1), 147-157.

Wattanaphan, P. (2012). *Studies and Prevention of Carbon Steel Corrosion and Solvent Degradation During Amine-Based CO_2 Capture from Industrial Gas Streams.* Faculty of Graduate Studies and Research, University of Regina.

Williams, I. (1937). Swelling and Solvation of Rubber in Different Solvents. *Ind. Eng. Chem., 29*(2), 172-174.

Wright, D. (2001). *Failure of Plastics and Rubber Products: Causes, Effects and Case Studies Involving Degradation*: Rapra Technology.

Zhang, P., He, J., & Zhou, X. (2008). An FTIR standard addition method for quantification of bound styrene in its copolymers. *Polym. Test., 27*(2), 153-157.

Zhao, Q., Li, X., & Gao, J. (2008). Surface degradation of ethylene‚Äìpropylene‚Äìdiene monomer (EPDM) containing 5-ethylidene-2-norbornene (ENB) as diene in artificial weathering environment. *Polym. Degrad. Stab., 93*(3), 692-699.

APPENDIX

Table A1 Study of mass change of raw elastomers after immersion for 30 days at 40 °C

Elastomers	MEA concentration (M)	CO_2 loading ($molCO_2$/ molMEA)	Mass Before (g)	Mass After (g)	Mass Change (%)	Average Mass Change (%)	S.D.
IIR	3	0	2.0844	2.0845	0.005	0.012	0.006
			2.1926	2.1929	0.014		
			2.383	2.3834	0.017		
	5	0	2.0326	2.0327	0.005	-0.005	0.008
			2.1567	2.1565	-0.009		
			1.9767	1.9765	-0.010		
	7	0	2.0102	2.0096	-0.030	-0.036	0.008
			2.0716	2.0709	-0.034		
			2.2341	2.2331	-0.045		
	5	0.15	2.2592	2.2591	-0.004	0.000	0.005
			2.0149	2.015	0.005		
			1.9522	1.9522	0.000		
	5	0.25	2.2902	2.2902	0.000	0.017	0.021
			1.9791	1.9799	0.040		
			2.1696	2.1698	0.009		
	5	0.5	2.2589	2.2593	0.018	0.020	0.016
			1.9559	1.956	0.005		
			1.93	1.9307	0.036		
NR	3	0	2.2705	2.6195	15.371	15.063	1.369
			2.1923	2.5486	16.252		

			2.0146	2.2879	13.566		
	5	0	2.2276	2.5155	12.924	12.916	0.778
			1.9474	2.214	13.690		
			2.1418	2.4017	12.135		
	7	0	2.2613	2.6195	15.840	15.286	0.705
			2.1444	2.4773	15.524		
			2.0114	2.3029	14.492		
	5	0.15	1.9015	1.9493	2.514	3.118	0.656
			2.2118	2.2787	3.025		
			2.1696	2.2524	3.816		
	5	0.25	2.1748	2.2369	2.855	2.627	0.505
			2.1369	2.2005	2.976		
			2.1091	2.1523	2.048		
	5	0.5	2.161	2.1851	1.115	1.117	0.421
			2.224	2.2395	0.697		
			2.1055	2.1379	1.539		
EPDM	3	0	2.1148	2.1166	0.085	0.170	0.076
			1.9296	1.9333	0.192		
			2.0236	2.0283	0.232		
	5	0	2.1842	2.1929	0.398	0.490	0.260
			2.156	2.1729	0.784		
			1.7324	1.7374	0.289		
	7	0	2.0683	2.1081	1.924	1.020	0.889
			2.1528	2.1741	0.989		
			1.6373	1.6397	0.147		
	5	0.166	2.1667	2.1919	1.163	0.696	0.407
			2.1055	2.1143	0.418		

			2.0372	2.0475	0.506		
	5	0.264	2.1233	2.1492	1.220	0.876	0.451
			1.8016	1.8082	0.366		
			2.2236	2.2468	1.043		
	5	0.5	1.9824	1.9903	0.399	0.938	0.531
			1.9712	1.99	0.954		
			2.1023	2.133	1.460		
SBR	3	0	2.2203	2.2535	1.495	1.194	0.262
			2.1841	2.2074	1.067		
			1.9926	2.0129	1.019		
	5	0	2.2482	2.3152	2.980	3.223	0.776
			2.1853	2.2747	4.091		
			2.0753	2.1292	2.597		
	7	0	1.9393	2.0719	6.838	5.227	1.447
			2.2484	2.3565	4.808		
			2.5018	2.6028	4.037		
	5	0.15	2.1825	2.1538	-1.315	-1.879	0.908
			2.5931	2.5172	-2.927		
			2.2637	2.2321	-1.396		
	5	0.25	2.0447	2.0013	-2.123	-2.574	0.400
			2.1089	2.0481	-2.883		
			2.3527	2.2888	-2.716		
	5	0.5	2.288	2.1928	-4.161	-3.482	0.965
			2.101	2.0189	-3.908		
			2.1461	2.0951	-2.376		

Table A2 Study of mass change of commercial seal material after immersed in 5 M MEA with 0.5 molCO_2/molMEA for 30 days

Material	Temperature (°C)	Mass Before (g)	Mass After (g)	Mass Change (%)	Average Mass Change (%)	S.D.
EPDM	40	3.6661	3.75	2.289	2.194	0.082
		3.6389	3.7171	2.149		
		3.6387	3.7167	2.144		
	120	3.6328	5.2364	44.142	44.314	0.179
		3.6612	5.2904	44.499		
		3.7009	5.3404	44.300		
IIR	40	3.6738	3.7611	2.376	2.287	0.219
		3.6863	3.7614	2.037		
		3.672	3.7619	2.448		
	120	3.713	5.2912	42.505	43.073	0.571
		3.7023	5.3182	43.646		
		3.6979	5.2905	43.068		
PTFE	40	5.5007	5.5011	0.007	0.006	0.017
		5.4578	5.459	0.022		
		5.5057	5.505	-0.013		
	120	5.4831	5.4968	0.250	0.180	0.080
		5.3993	5.4043	0.093		
		5.4215	5.4322	0.197		

Table A3 Study tensile strength of commercial seal material after immersed in 5 M MEA with 0.5 molCO_2/molMEA for 30 days

Material	Temperature (°C)	Thickness (in)	Width (in)	Peak load (lbf)	Peak stress (psi)	avg	SD
EPDM	-	0.063	0.25	10.4	660.3	660.3	-
	40	0.0648	0.25	8.2	506	506	-
	120	0.063	0.25	2.7	171.4	169.3	3.637
		0.063	0.25	2.6	165.1		
		0.063	0.25	2.7	171.4		
IIR	-	0.063	0.25	6.6	419	419	-
	40	0.0645	0.252	7.3	449	449	-
	120	0.063	0.25	2.3	146	150	3.464
		0.063	0.25	2.4	152		
		0.063	0.25	2.4	152		
PTFE	-	0.064	0.257	48.9	2967	2967	-
	40	0.0638	0.255	49.3	3030	3030	-
	120	0.064	0.256	50.3	3070	3070	-

Table A4 Study hardness of commercial seal material after immersed in 5 M MEA with 0.5 molCO_2/molMEA for 30 days

Material	Temperature (°C)	Hardness	avg	S.D.
EPDM	-	78.6	78.6	-
	40	77.6	77.6	-
	120	47.6	47.6	0.200
		47.4		
		47.8		
IIR	-	76.6	76.6	-
	40	76.6	76.6	-
	120	46.8	47.7	0.902
		47.6		
		48.6		
PTFE	-	98.2	98.2	-
	40	98.8	98.8	-
	120	98.6	98.6	-